의학석사 학위논문

전립선 암에서 HIF 매개 저산소 반응의 균형조절에 있어 NDRG3의 역할에 관한 연구

Role of NDRG3 in counterbalancing the HIF-mediated hypoxic responses in prostate cancer

2018년 2월

서울대학교 대학원

의과학과 의과학전공

이 가 영

A thesis of the Degree of Master of Science

Role of NDRG3 in counterbalancing the HIF-mediated hypoxic responses in prostate cancer

전립선 암에서 HIF 매개 저산소 반응의 균형조절에 있어 NDRG3의 역할에 관한 연구

February 2018

The Department of Biomedical Sciences,

Seoul National University

College of Medicine

Ga Young Lee

ABSTRACT

Hypoxia-inducible factors (HIFs) and N-MYC downstream-regulated gene 3 (NDRG3) expressions are oxygen-dependently regulated by the prolyl-hydroxylase domain enzymes (PHDs). The roles of NDRG3 in cellular adaptation to hypoxia is little known, whereas those of HIFs are well understood. In this study, we investigated how NDRG3 affects the hypoxic response in prostate cancer cells. Compared with HIF-1α, the hypoxic induction of NDRG3 was observed at a later phase. NDRG3 reduced the hypoxic expression of HIF-1α by inhibiting the AKT-driven translation of HIF1A mRNA. In addition, NDRG3 functionally inhibited HIF-1 by dissociating the coactivator p300 from HIF-1α. Accordingly, NDRG3 may fine-tune the HIF-1 signaling pathway to cope with a long-term hypoxia. Of diverse effects of HIF-1α on cancer progression, the hypoxia-induced cell migration was investigated. In trans-well chambers, NDRG3 negatively regulated migration and invasion of prostate cancer cells under hypoxia. An informatics analysis using GEO revealed that NDRG3 downregulation is associated with prostate cancer metastasis and high

expression of HIF-1 downstream genes. In cancer tissue arrays, NDRG3 expression was lower in prostate cancer tissues with 8 or more Gleason score and inversely correlated with HIF-1α expression. Therefore, NDRG3 seems to have an anti-metastatic function in prostate cancer under hypoxic microenvironment.

Key words: hypoxia, HIF-1α, prostate cancer, NDRG3, AKT, metastasis

Student Number: 2015-23242

CONTENTS

LIST OF FIGURES

LIST OF ABBREVIATION

ARNT: aryl hydrocarbon receptor nuclear translocator

EMT: epithelial-mesenchymal transition

FIH: factor inhibiting HIF

GSEA: gene set enrichment analysis

HIF-1α: hypoxia-inducible factor 1

HRE: hypoxia response element

IHC: immunohistochemistry

Luc: luciferase activity

NDRG3: N-myc downstream-regulated gene 3

PI3K: phosphoinositide 3-kinase

PHD: prolyl hydroxylase domain

pVHL: Von hippel-lindau protein

INTRODUCTION

Metazoan cells maintain oxygen homeostasis through balancing between mitochondrial oxygen consumption and external oxygen supply. Disruption in this balance results in energy depletion or oxidative injury, which may lead to various diseases including cancer (Semenza, 2001). Hypoxia-inducible factor 1 and 2 (HIF-1/2), which are bHLH-PAS family transcription factors composed of α and β subunits, play key roles in keeping oxygen homeostasis (Semenza, 1999; Wang *et al.*, 1995). Although hypoxia is lethal to both normal and cancer cells, cancer cell rewires its key pathways such as oxygen transport, angiogenesis, and metabolism, and succeeds to not only adapt to hypoxic conditions, but also exploits hypoxia as a driving force of tumor growth (Harris, 2002).

HIF-1α expression is tightly regulated by the prolyl hydroxylases PHD1-3 whose activities are dependent on the ambient oxygen tension. In aerobic conditions, PHDs hydroxylate the Pro-402 and Pro-564 residues on the ODD domain in HIF-1α, allowing the von Hippel-Lindau protein (pVHL) E3 ligase complex to ubiquitinate

HIF-1α and to promote proteasomal degradation (Huang *et al.*, 1998; Kaelin *et al.*, 2008; Semenza, 2004). In oxygen-deficient conditions, however, HIF-1α is stabilized because PHDs are inactivated. HIF-1α dimerizes with HIF-1β/ARNT in the nucleus and expresses hundreds of its downstream genes (Jaakkola *et al.*, 2001; Schofield *et al.*, 2004). The activity of HIF-1α is oxygen-dependently regulated as well by FIH-1 (factor inhibiting HIF-1), which inhibits HIF-1α from binding with its co-activators CBP/p300 by hydroxylating Asn-803 residue in the HIF-1α C-terminal transactivation domain (CAD) (Lando *et al.*, 2002a; Lando *et al.*, 2002b).

Besides the oxygen-dependent regulation, HIF-1α expression is also determined at the translational step, which is activated by the PI3K-AKT-mTOR pathway. This pathway is highly activated in prostate cancer cells because of the deletion of the *PTEN* gene, so HIF-1α is frequently overexpressed in prostate cancer (Shukla *et al.*, 2007; Zhong *et al.*, 2000).

The NDRG family, which is composed of four members (NDRG1-4), has been suggested to govern essential cellular activities due to its high conservation in different species (Zhou *et al.*, 2001).

Although α/β hydrolase fold domain is present in all four members, the catalytic triad is missing several residues, disabling their functions as hydrolases (Melotte *et al.*, 2010; Shaw *et al.*, 2002). Nevertheless, NDRGs have been reported to play important roles in various cellular functions such as cell differentiation, immune systems, endocrine signaling, and nervous systems (Qu *et al.*, 2002). NDRGs have also been reviewed to display tumor-suppressive behaviors in various cancers, suggesting them as good prognostic markers, and they seem to be deeply engaged in the hypoxia-induced reprogramming of cancer metabolism (Lee *et al.*, 2016).

Recently, NDRG3 was revealed as another target for the PHD oxygen sensor (Lee *et al.*, 2015). Similar to HIF-1α, NDRG3 is prolyl-hydroxylated under normoxia by PHD2, poly-ubiquitinated by pVHL, and degraded through the proteasomal pathway. NDRG3 becomes stable under hypoxia because this degradation process is blocked due to absence of oxygen substrate. If hypoxia persists, accumulated lactate interferes with the interaction between NDRG3 and PHD2. Therefore, lack of oxygen and lactate production both facilitate the stabilization of NDRG3 in a long-term hypoxia. Functionally, NDRG3 is regarded to prolong hypoxic responses such as angiogenesis

and cell growth in persisting hypoxia, whereas short-lived HIF-1α takes part in immediate hypoxic responses. However, I had a question about whether HIF-1α and NDRG3 cooperatively work for cellular adaptation to hypoxia.

In this work, I investigated the cross-talk between HIF-1α and NDRG3 in prostate cancer cells. Furthermore, I examined the consequence of hypoxic induction of NDRG3 in cancer metastasis.

MATERIALS AND METHODS

Cell Culture

The PC3 and DU145 cell lines were purchased from the Korean Cell Line Bank (Seoul, Korea). PC3 and DU145 were maintained in RPMI1640 medium supplemented with 10% heat-activated fetal bovine serum and 1% penicillin and streptomycin. Incubator gas tension was maintained at 5% CO_2/21%O_2 for normoxic conditions and 5% CO_2/1%O_2 for hypoxic conditions.

Antibodies and reagents

Culture media and fetal bovine serum was purchased from Sigma-Aldrich (St. Louis, MO). Anti-HIF-1α antibody was generated in rabbits using bacterially expressed fragment containing amino acids 418-698 of human HIF-1α (Chun *et al.*, 2000). Anti-NDRG3 antiserum was raised from rabbits (New Zealand White) through a commercial facility (AbClon, Seoul, Korea). Rabbits were immunized with Keyhole limpet haemocyanin (KLH)-conjugated NDRG3 peptide

(HSTSSSLGSGESPFSRSVTSNQSDGTQESCESPDVLDRHQTMEVSC). Antibodies against phospho-AKT (S473), total AKT and Myc-tag were purchased from Cell Signaling (Danvers, MA); anti-Gal4(DBD), anti-β-tubulin, anti-GFP and HRP-conjugated secondary antibodies from Santa Cruz Biotechnology (Santa Cruz, CA); anti-HA from Roche Diagnostics (Mannheim, Germany); anti-HIF-2α from Novus Biologicals (Littleton, CO). MK2206 was purchased from Selleckchem and other chemicals from Sigma-Aldrich.

Preparation of plasmids, short interfering RNAs (siRNAs) and transfection

The cDNA of NDRG3 was cloned by reverse transcription and PCR using pfu DNA polymerase, and the cDNA was inserted into the MYC-tagged vector by blunt-end ligation. The sequence of siRNA targeting NDRG3 (NM_032013) was 5'-AGAUCAAACCACUUCUAAA UGAUAA-3' (siNDRG3), siRNA targeting HIF-1α was 5'-CAAAGUUA AAGCAUCAGGUUCCUUCUU-3' (siHIF-1α), siRNA targeting HIF-2α was 5'-GGGUUACUGACGUGTAAAUGCTGGU-3' (siHIF-1α), and the the non-targeting siRNA sequence was 5'-AUGAACGUGAA

UUGCUCAATT-3'. Gal4-CAD (HIF-1α a.a.776-826), Gal4-CAD-N803A, Gal4-NAD (HIF-1α a.a 498-603), and VP16-p300 CH1 plasmids were constructed, as previously described (To *et al.*, 2005). For transient gene silencing or protein expression, 40% confluent cells were transfected with plasmids or siRNAs using Lipofectamine 3000 or Lipofectamine RNA iMAX, respectively. The transfected cells were stabilized for 48 hours before being used in experiments.

Reporter gene construction and luciferase assay

The luciferase reporter genes containing the hypoxia response element (HRE) of the erythropoietin enhancer or the mutated HRE were kindly given by Dr. Eric Huang (University of Utah). To determine the cap-dependent translation of HIF-1α, the HIF-1α 5'UTR (1-284) segment was cloned using RT-PCR, and was inserted between thymidine kinase promoter and luciferase in the GL3 plasmid, as previously described (Shin *et al.*, 2010). PC3 or DU145 cells were co-transfected with 1μg of the reporter plasmid, 1μg of the CMV-β-galactosidase plasmid, 40 nM NDRG3 siRNAs or 1μg of the NDRG3 plasmid. After stabilized for 48 hours, cells were incubated in

1% O_2 or 21% O_2 for 24 hours, and luciferase activities in cell lystates were measured using Lumat LB9507 luminometer (Berthold Technologies, Bad Wildbad, Germany). The specific reporter activity was calculated by dividing luciferase activity by β-galactosidase activity.

Gal4-reporter and mammalian two-hybrid assays

To evaluate HIF-1α CAD and NAD activities, PC3 and DU145 cells were co-transfected with 100 ng of Gal4-CAD(or CAD N803A) plasmid, 100 ng of Gal4-Luc plasmid, 500 ng of β-galactosidase plasmid, 40 nM NDRG3 siRNA, or 1 μg of MYC-NDRG3 plasmid using lipofectamine 3000. For mammalian two-hybrid assays, PC3 and DU145 cells were co-transfected with 100 ng of Gal4-CAD plasmid, 100 ng of Gal4-Luc plasmid, 500 ng of CH1-VP16 plasmid, 500 ng of CMV-β-galactosidase plasmid, 40 nM NDRG3 siRNA, or 1 μg of MYC-NDRG3 plasmid using lipofectamine 3000. After stabilized for 48 hours, cells were incubated in 1% O_2 or 21% O_2 for 24hours, and luciferase activities in cell lysates were measured using Lumat LB9507 luminometer (Berthold Technologies, Bad Wildbad, Germany). Thespecific reporter activity was calculated by dividing luciferase

activity by β-galactosidase activity.

Immunoblotting and Immunoprecipitation

Cell lysates were separated on SDS-polyacrylamide gels, and transferred to Immobilon-P membranes (Millipore; Bedford, MA). Membranes were blocked with a Tris/saline solution containing 5% skim milk and 0.1% Tween-20 for 1 hour, and incubated with a primary antibody overnight at 4°C. Membranes were incubated with a horseradish peroxidase–conjugated secondary antibody for 1 hour, and visualized using the ECL kit (Thermo; Rockford, IL). To analyze protein interactions, cell lysates were incubated with anti-HA or anti-MYC antibody for 4 hours at 4°C, and the immune complexes were precipitated with protein A/G beads (Santa Cruz, CA). Precipitated proteins were eluted in a denaturing 2xSDS sample buffer, loaded on SDS-PAGE, and immunoblotted.

Cell migration and invasion assays

Transfected PC3 or DU145 cells were cultured in 6.5-mm

transwell inserts with 8 μm pore size, coated with either collagen I or 0.5 mg/μL of growth factor-reduced Matrigel, purchased from Corning Life Science (Acton, MA). Cells were seeded into the upper chambers in 100 μL of FBS-free medium, while 10% FBS-containing medium was placed in the lower chambers as chemo-attractant, and incubated in either 1% O_2 or 21% O_2 for 24 hours. Cells on the lower surface of the transwell inserts were fixed in 4% formaldehyde and stained with hematoxylin and eosin, and four high-power independent fields in each membrane were counted.

Quantitative RT-PCR

Total RNA was isolated using TRIZOL reagent (Invitrogen; Carlsbad, CA), and cDNA synthesis was carried out in a reaction mixture (Promega, Madison, WI) containing M-MLV Reverse Transcriptase, RNase inhibitor, dNTP, and random primers at 46°C for 1 h. Quantitative real-time PCR on 96-well optical plates was performed in the qPCR Mastermix (Enzynomics, Daejeon, Korea), and fluorescence emitting from dye-DNA complex was monitored in CFX Connect Real-Time Cycler (BIO-RAD, Hercules, CA). The mRNA

values of targeted genes were calculated relative to GAPDH expression. All reactions were performed in triplicate. The nucleotide sequences of PCR primers are summarized in Table 1.

Immunohistochemistry in human prostate cancer tissues

Human prostate cancer tissue microarrays were purchased from SuperBioChips Lab (Seoul, South Korea). Tumor staging was defined according to the AJCC cancer staging manual (7th edition). Paraffin-fixed tissue slides were incubated in 60°C oven for 1 hour to remove paraffin, and were autoclaved in retrieval antigen solution. After treatment with 3% H_2O_2, tissue sections were incubated with primary antibodies (anti-NDRG3 and anti-HIF-1α) overnight at 4°C, followed by biotinylated secondary antibodies for 1 hour at 25°C. The immune complexes were visualized using Vectastatin ABC kit (Vector Laboratories, Burlingame, CA), and counterstained with hematoxylin for 10 minutes. Protein expression levels were analyzed by counting positively stained cells on four independent high-power fields on each slide.

Informatics analysis

The normalized data set GSE6919 for prostate cancer was imported from Gene Expression Omnibus, which the total patients (n=167) were categorized into four groups: normal prostate tissue free of any pathological alterations (n=17), normal prostate tissue adjacent to tumor (n=59), primary prostate tumor (n=66) and metastatic prostate tumor (n=25). For mRNA expression analysis, normalized values of 57107_at (corresponding to NDRG3) in each group were compared between the three groups; normal prostate tissue adjacent to tumor, primary prostate tumor and metastatic prostate tumor. Group consisted of 'normal prostate tissue free of any pathological alterations' (n=18) was excluded from mRNA analysis. For gene set enrichment analysis (GSEA), a formatted GCT file was used as input for the GSEA algorithm v2.0 (available from: http://www.broadinstitute.org/gsea). For grouping the GSE6919 data set, the values of the 57107_at (corresponding to NDRG3) were used as criteria standard for low expression and high expression group. The phenotype and the default parameters were used with the results that the Pearson correlation was computed to rank the genes.

Statistics

All data were analyzed using Microsoft Excel 2013 software or Graph pad Prism 5 software, and results were expressed as means and standard deviations. I used the unpaired, two-sided Student t-test to compare protein levels, luciferase activities, and cell numbers. Statistical significances were considered when P values were less than 0.05. Protein or mRNA expression correlations were analyzed using a Spearman's p statistics. Survival rate analysis were performed by drawing curves and calculating log-rank P test using The Kaplan-Meier method.

RESULTS

NDRG3 and HIF-α reciprocally regulate each other in the protein level.

I first examined the temporal patterns of NDRG3 and HIF-1/2α expressions during hypoxia. As was reported (Ginouves *et al.*, 2008), HIF-1/2α levels in prostate cancer cells increased as early as 4 hours after hypoxia and subsided after 16 hours. In contrast, NDRG3 started to be induced 16 hours after hypoxia and its level was gradually increased along increasing time of hypoxia (Fig. 1A). I noted that HIF-1/2α expressions precede NDRG3 expression and that NDRG3 expression precedes a gradual decline of HIF-1/2α. Given such kinetic patterns in HIF-1/2α and NDRG3 expressions, I suspected a reciprocal regulation between them. When HIF-1α or HIF-2α was knocked down in prostate cancer cells, the hypoxic induction of NDRG3 was weakened (Fig. 1B). Indeed, the HIF-dependent expression of NDRG3 has been demonstrated by a recent report (Lee *et al.*, 2015). Lee et al. suggested that HIFs promote lactate production by upregulating a series of glycolytic enzymes and the accumulated lactate potentiates the hypoxic stabilization of NDRG3 by inhibiting the PHD docking to

NDRG3. On the other hand, I found that the hypoxic induction of HIF-1/2α was potentiated by NDRG3 knockdown but weakened by NDRG3 overexpression (Fig. 2A). Furthermore, qRT-PCR analyses revealed that the mRNA levels of HIF-downstream genes PDK1 and BNIP3 in prostate cancer cells were significantly increased under hypoxia by NDRG3 knockdown (Fig. 3A). While hypoxia persists, accordingly, HIFs upregulate NDRG3 and in turn NDRG3 inhibits HIFs. NDRG3 may function to control the HIF-mediated hypoxic response through a negative feed-back loop.

Cap-dependent translation of HIF-1α is reduced by NDRG3.

I next proceeded to determine how NDRG3 downregulates HIF-1α and HIF-2α. Since NDRG3 knockdown did not increase HIF-1α or HIF-2α mRNA levels (Fig. 4A), NDRG3 may regulate HIF-1/2α at the post-transcriptional level. Next, I compared the oxygen-dependent degradation rates of HIF-1/2α proteins, and found that the stabilities of HIF-1/2α proteins were not significantly altered by NDRG3 knockdown (Fig. 5A, Fig. 5B). Subsequently, the effect of NDRG3 on HIF-1/2α protein syntheses was examined. The rate of *de novo* protein synthesis

was analyzed in the presence of MG132 which blocks HIF-1/2α degradation. Given that the synthesis rates of HIF-1/2α proteins were enhanced by NDRG3 knockdown (Fig. 6A, Fig. 6B), NDRG3 is likely to control the translation of HIF-1/2α mRNA. I checked the inhibitory function of NDRG3 on HIF-1α translation using the *HIF1A*_5'UTR-luciferase reporter, which reflects the cap-dependent translation of HIF-1α. Luciferase activity was largely increased by NDRG3 knockdown in both normoxia and hypoxia (Fig. 7A). This result further supports my notion that NDRG3 negatively regulates *de novo* synthesis of HIF-1α protein.

NDRG3 inhibits the AKT-dependent syntheses of HIF-1/2α proteins.

The cap-dependent translation of HIF-1/2α in prostate cancer cells has been reported to be promoted through the PI3K-AKT-mTOR pathway (Khatua *et al.*, 2003; Semenza, 2003; Zhong *et al.*, 2000). Therefore, I tested the possibility that NDRG3 controls such a pathway, and found that NDRG3 negatively regulates the AKT phosphorylation in prostate cancer cells (Fig. 8A). Furthermore, HIF-1α and HIF-2α syntheses induced by NDRG3 knockdown were abolished by an AKT

inhibitor MK-2206 (Fig. 8B). As shown in the *HIF1A*_5'UTR-lucifease reporter system, the cap-dependent translation of HIF-1α was significantly decreased by MK-2206 (Fig. 8C). Taken together, NDRG3 might function to control HIF-1/2α expression by inhibiting the AKT-dependent translation of their mRNAs.

NDRG3 inhibits the HIF-driven transcription of the HRE promotor.

To examine whether NDRG3 controls the HIF-driven gene expression under hypoxia, the HRE-luciferase reporter plasmid, which contains the hypoxia response element (HRE) in the erythropoietin enhancer region, was adopted. The hypoxic enhancement of the reporter activity was augmented by NDRG3 knockdown (Fig. 9A) but attenuated by NDRG3 overexpression (Fig. 9B). As the mutated HRE reporter activity was constant regardless of NDRG3 expression, NDRG3 controls the reporter activity by specifically regulating HIF-1/2. To examine if NDRG3 knockdown enhances the HIF-driven transcription through the AKT signaling, I analyzed the reporter activity in the presence of MK-2206. The NDRG3 knockdown-induced increase in the luciferase activity was significantly, but not fully, diminished by MK-2206 (Fig.

9C). This result suggests that the NDRG3 inhibition of the HIF-driven transcription is partially attributed to the reduction in AKT-dependent synthesis of HIF-1/2α proteins. In addition to AKT inhibition, however, another mechanism may contribute to the functional inhibition of HIF-1/2α by NDRG3.

NDRG3 functionally inhibits HIF-1 by interfering with p300 binding to HIF-1α.

Next, I tested the possibility that NDRG3 controls the hypoxic activation of HIF-1α_CAD (the transactivation domain at the C-terminus) using the Gal4 reporter system, which contains the Gal4 DNA-binding domain/HIF-1α_CAD fusion gene and the Gal4 promoter-luciferase fusion gene. Because the Gal4-CAD fusion protein is constantly expressed regardless of the oxygen tension (Fig. 10A), this reporter system can reflect the transcriptional activity of HIF-1α irrespective of HIF-1α stability. Aside from the change in protein synthesis, the transcriptional activity of HIF-1α was also found to be elevated by NDRG3 knockdown, but to be repressed by NDRG3 overexpression (Fig. 10B). HIF-1α_CAD is known to be

oxygen-dependently inactivated by FIH, which enzymatically hydroxylates the N803 residue of CAD (Lando *et al.*, 2002b). To examine whether NDRG3 regulates such an action of FIH, I measured the activity of the Gal4-CAD_N803A mutant, which is not regulated by FIH. Unexpectedly, NDRG3 was found to control the CAD activity irrespective of the N803 hydroxylation by FIH (Fig. 10C). Next, I checked the interaction between the HIF-1α_CAD and the CH1 domain of p300, which is an essential process for the HIF-driven transcription. For this analysis, I adopted the mammalian two-hybrid system, which contains Gal4 promoter-luciferase, Gal4-CAD, and VP16-CH1 plasmids. Consequently, the CAD-CH1 interaction was markedly enhanced by NDRG3 knockdown but almost completely inhibited by NDRG3 overexpression (Fig. 10D), strongly indicating that NDRG3 interferes with the p300 binding to HIF-1α. To confirm this effect of NDRG3, co-immunoprecipitation was performed. GFP-HIF-1α and HA-p300 was co-expressed in PC3 cells and the cell lysates were immunoprecipitated with anti-HA beads. With increasing expression of NDRG3, the interaction between HIF-1α and p300 was reduced (Fig. 10E). These findings suggest that NDRG3 represses the HIF-driven transcription by dissociating p300 from HIF-1α.

NDRG3 inhibits the hypoxia-induced migration and invasion of prostate cancer cells.

In a view-point of cancer, the hypoxia-induced cancer metastasis is regarded as one of the most important roles of HIF-1α. HIF-1α is known to induce cancer metastasis by expressing the EMT-inducing genes such as Twist and Snail (Imai *et al.*, 2003; Yang *et al.*, 2008a; Yang *et al.*, 2008b). Therefore, I proceeded to study the role of NDRG3 on cell migration and invasion in prostate cancer. In trans-well migration assay, cell migration under hypoxia was facilitated by NDRG3 knockdown but was attenuated by NDRG3 overexpression in PC3 cells (Fig. 11A) and DU145 cells (Fig. 11B). Furthermore, cell invasion was also found to be negatively regulated by NDRG3 in PC3 cells (Fig. 11C) and DU145 cells (Fig. 11D).

NDRG3 expression inversely correlates with metastasis and HIF-1α expression in human prostate cancer.

To investigate the role of NDRG3 in prostate cancer progression, NDRG3 mRNA levels in prostate cancer tissues were analyzed using the NCBI_GEO data set GSE6919. NDRG3 mRNA levels was

significantly lower in metastatic prostate cancer tissues than in primary cancer tissues or normal tissues (Fig. 12A). Based on the median value (961.25) of NDRG3 mRNA (Fig. 12B), prostate cancer tissues were divided into two groups, NDRG3_Low and NDRG3_High. I performed gene set enrichment analysis (GSEA) using the HIF-1 downstream gene set HIF1_TFPATHWAY, and found that HIF-1 downstream genes are significantly enriched in the NDRG3_Low group (Fig. 12C). These informatics analyses prompted us to check the NDRG3 protein levels in prostate cancer tissues obtained from patients. Immunohistochemical analyses (IHC) showed that NDRG3 expression in prostate cancer was gradually reduced along increasing Gleason score (Fig 13A). In contrast, HIF-1α expression was found to be increased in cancer with high Gleason score, which is consistent with other reports (Boddy *et al.*, 2005; Zhong *et al.*, 1998). Furthermore, patients in the NDRG3_Low group tend to have lower disease-free survival rates than those in the NDRG3_High group, while patients in the HIF-1α_Low group showed higher survival rate (Fig. 13B). Pearson correlation analysis also showed a negative correlation between NDRG3 and HIF-1α protein expressions in prostate cancer tissues (Fig. 13C), further supporting the notion that NDRG3 is a negative regulator of HIF-1α. Taken together, I propose

that NDRG3 plays an anti-metastatic role in prostate cancer by antagonizing the HIF signaling pathway.

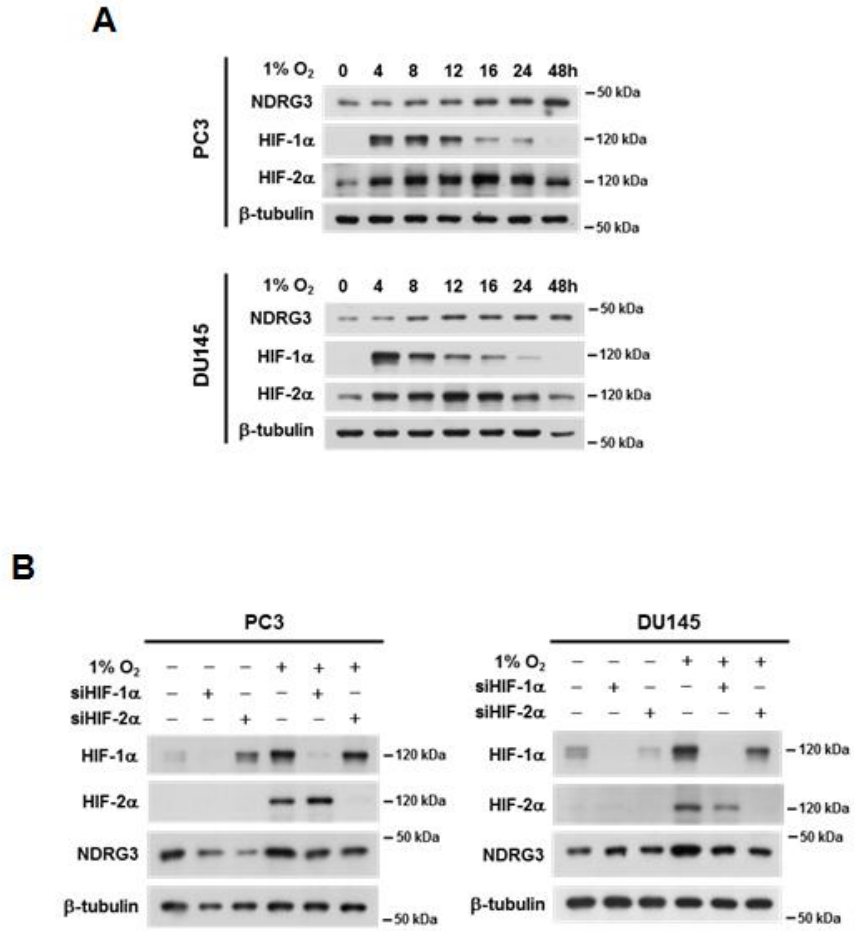
A
PC3
1% O2
0
4
8
12
16
24
48h
NDRG3
HIF-1α
HIF-2α
β-tubulin
50 kDa
120 kDa
DU145
B
PC3
DU145
1% O2
siHIF-1α
siHIF-2α
HIF-1α
HIF-2α
NDRG3
β-tubulin

Fig. 1. HIF-1α and HIF-2α protein level reduction in prolonged hypoxia is correlated with NDRG3 accumulation.

(A) PC3 and DU145 cells were incubated under hypoxia (1% O_2) for the indicated times, and subjected to Western blotting with anti-HIF-1α or anti-HIF-2α antibody. (B) PC3 and DU145 cells, which had been transfected with siRNAs silencing HIF-1α or HIF-2α, were incubated under normoxia or hypoxia for 24 hours, and subjected to Western blotting.

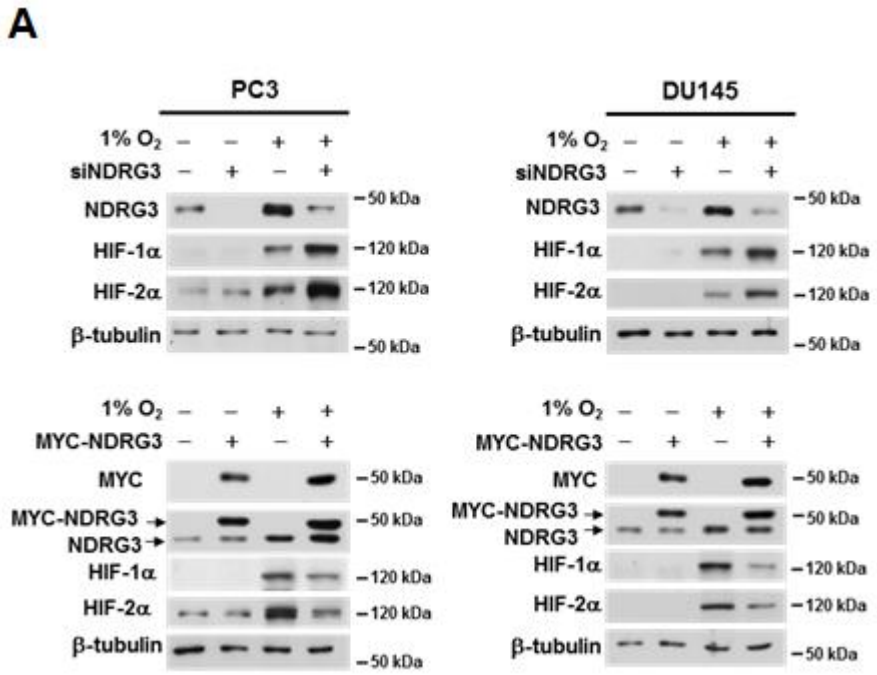

Fig. 2. NDRG3 is a negative regulator of HIF-1α and HIF-2α

(A) PC3 and DU145 cells, which had been transfected with NDRG3-silencing siRNA, were incubated under normoxia or hypoxia for 24 hours, and subjected to Western blotting.

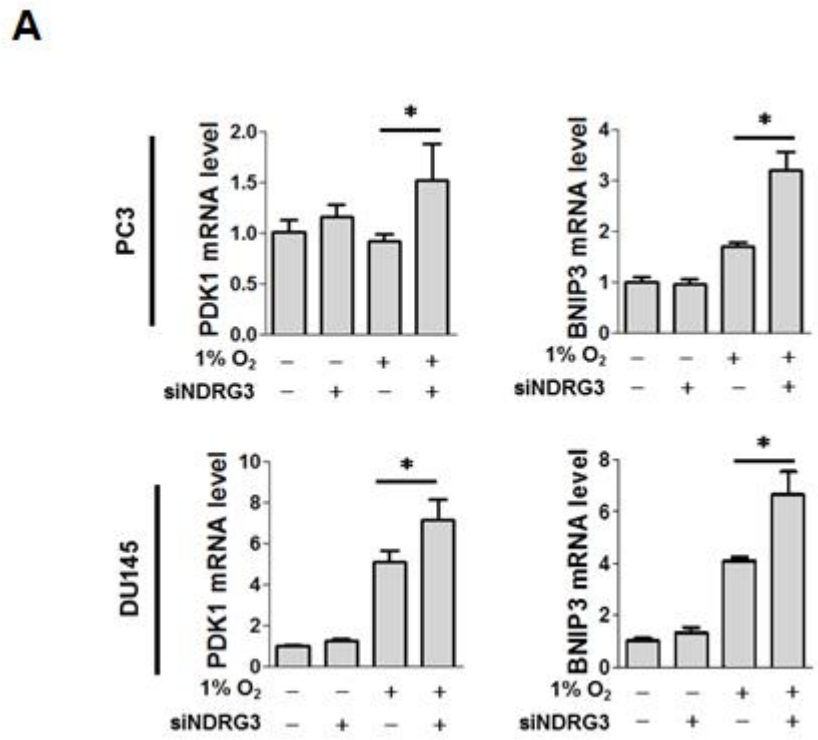

Fig. 3. NDRG3 knockdown promotes hypoxic induction.

(A) PC3 and DU145 cells, which had been transfected with NDRG3-silencing siRNA, were incubated under normoxia or hypoxia for 24 hours and lysed for RNA extraction. PDK1 and BNIP3 mRNA levels were measured by RT-qPCR. Each bar represents the mean + s.d. (n = 3) and * denotes $P < 0.05$ between the indicated groups.

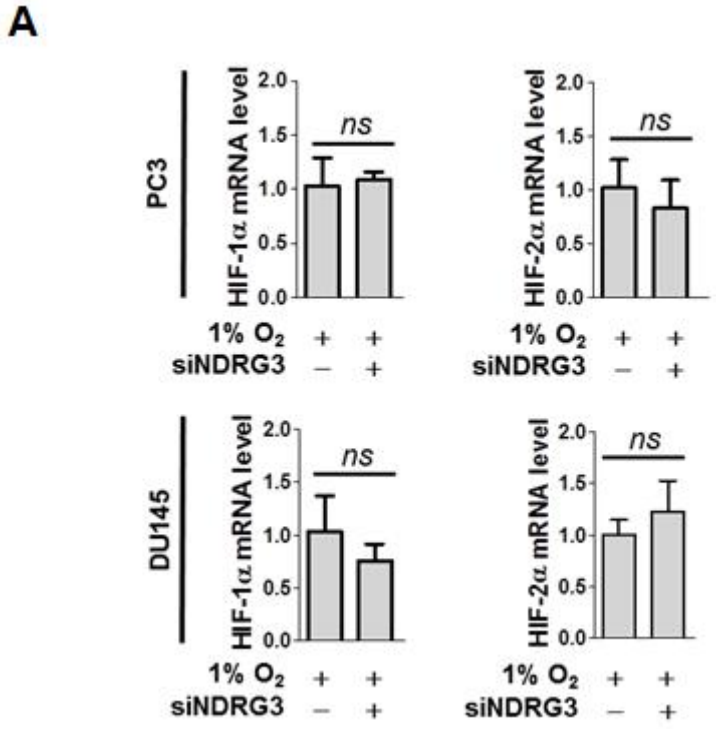

Fig. 4. HIF-1α and HIF-2α transcriptions are independent of NDRG3.

(A) PC3 and DU145 cells, which had been transfected with NDRG3-silencing siRNA, were incubated under hypoxia for 24 hours and subjected to RT-qPCR for measuring the mRNA levels of HIF-1α and HIF-2α (means + s.d., *n* = 3). *ns* denotes 'not significantly different'.

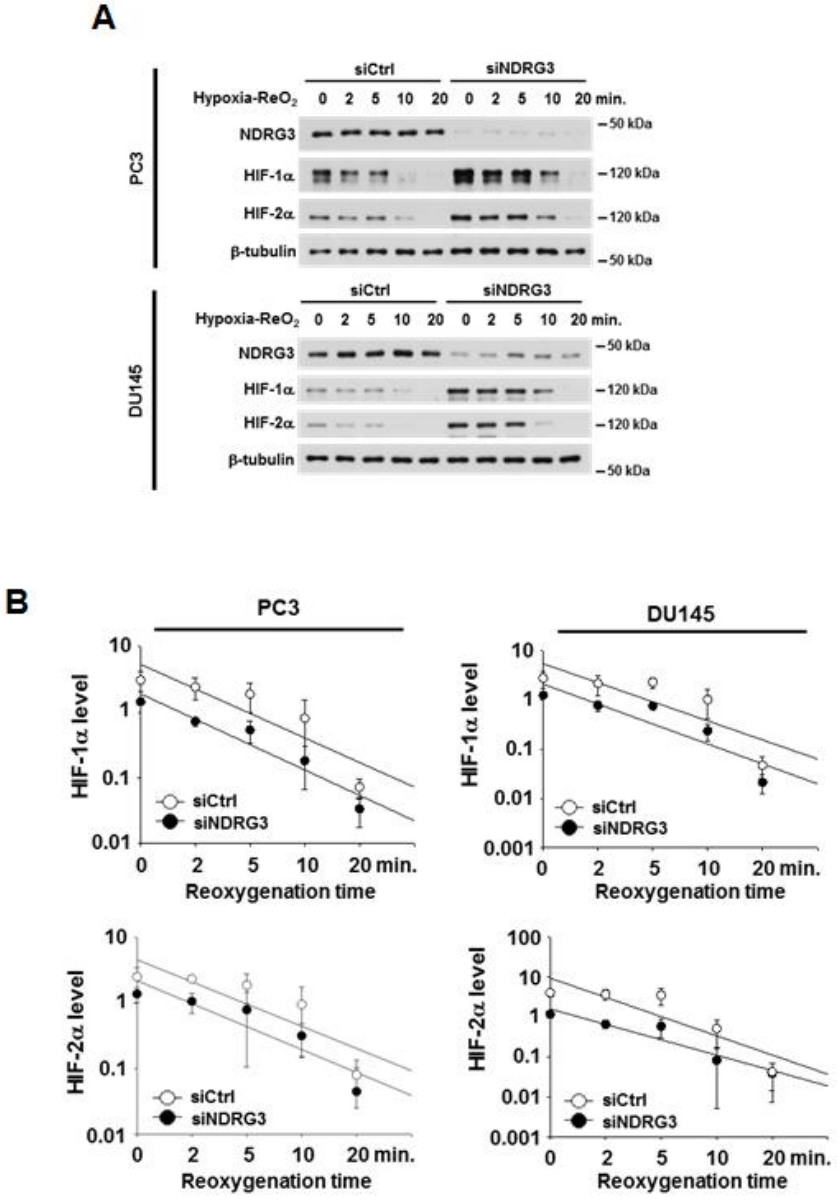
A
PC3
DU145
siCtrl
siNDRG3
Hypoxia-ReO2
0 2 5 10 20 0 2 5 10 20 min.
NDRG3
HIF-1α
HIF-2α
β-tubulin
50 kDa
120 kDa
B
PC3
DU145
HIF-1α level
HIF-2α level
siCtrl
siNDRG3
Reoxygenation time
0 2 5 10 20 min.

Fig. 5. HIF-1α and HIF-2α protein stabilities are not regulated by NDRG3.

(A) The transfected PC3 or DU145 cells were incubated under hypoxia for 8 hours, followed by re-oxygenation at 21% O_2. HIF-1α and HIF-2α proteins were immunoblotted. (B) Blots in Fig. 5A were quantified using the ImageJ program. Each symbol represent the mean ± s.d. (n = 3) and the linear regression was plotted using the SigmaPlot program.

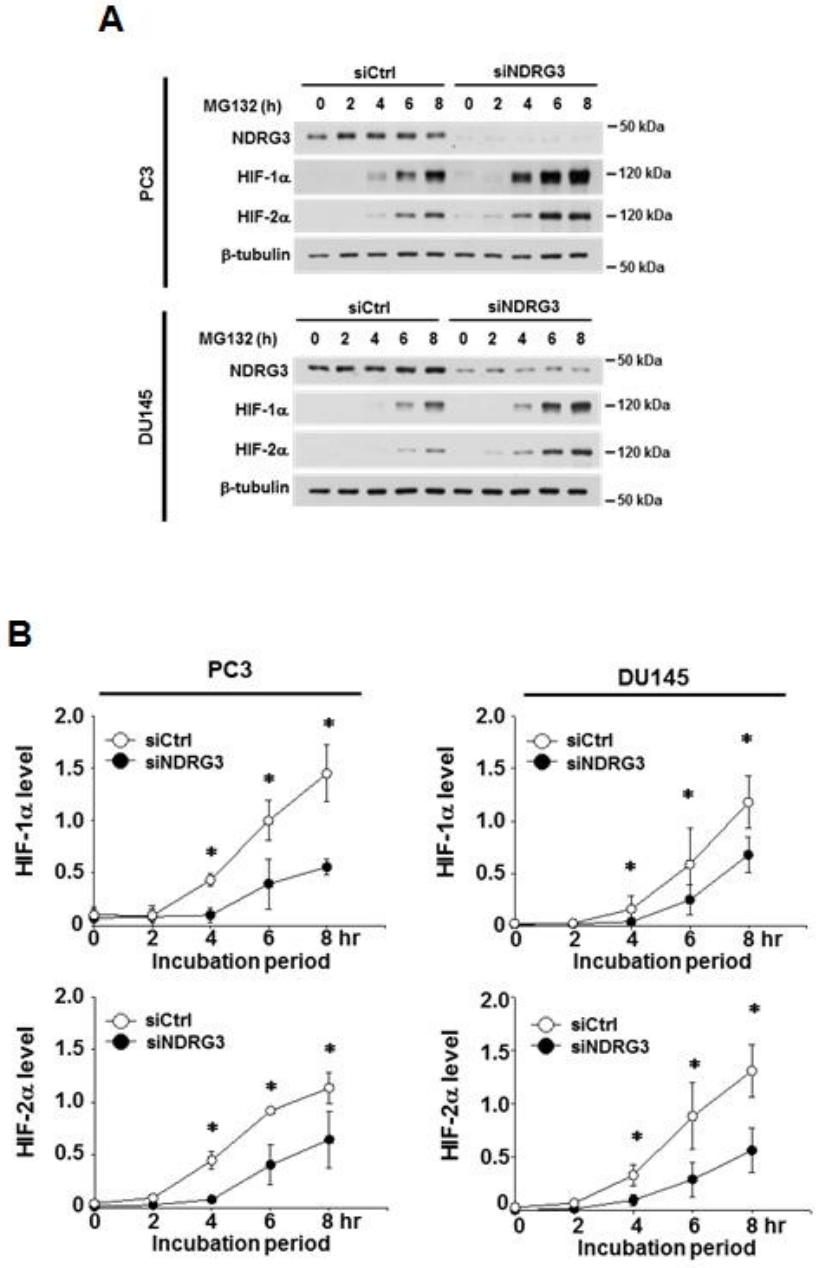
A
siCtrl
siNDRG3
MG132 (h)
0 2 4 6 8 0 2 4 6 8
PC3
NDRG3
HIF-1α
HIF-2α
β-tubulin
50 kDa
120 kDa
120 kDa
50 kDa
DU145
B
PC3
DU145
HIF-1α level
HIF-2α level
siCtrl
siNDRG3
Incubation period
0 2 4 6 8 hr

Fig. 6. NDRG3 knockdown increases HIF-1α and HIF-2α protein synthesis rates.

(A) The transfected PC3 or DU145 cells were incubated with 15 μM MG132 for the indicated times. (B) Western blot intensities were analyzed using ImageJ and normalized to β-tubulin intensities. Each symbol represent the mean ± s.d. (n = 3). * denotes $P < 0.05$ versus the siCtrl group at the corresponding time.

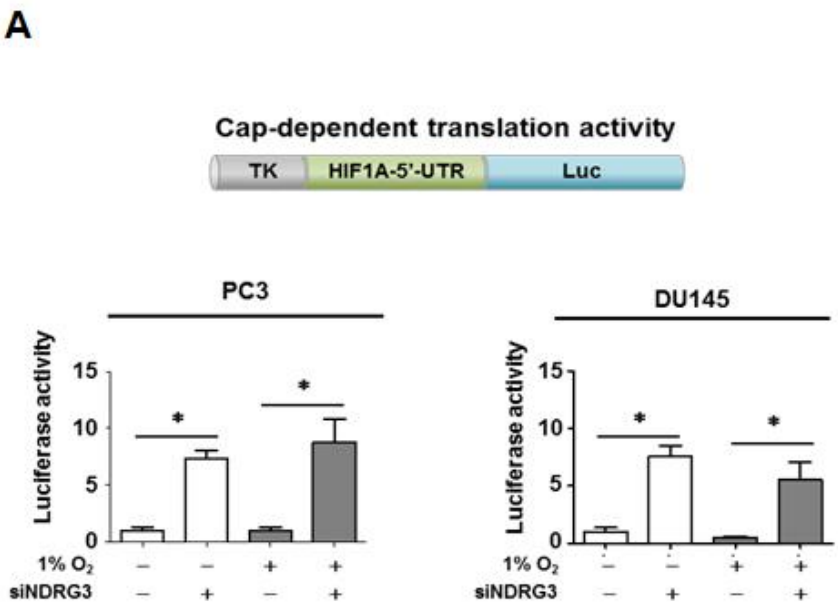

Fig. 7. Cap-dependent translation activity of HIF-1α is negatively regulated by NDRG3.

(A) PC3 or DU145 cells were cotransfected with the TK-HIF1A 5'UTR-luciferase plasmid, the CMV-β-galactosidase plasmid, and siCtrl or siNDRG3. After stabilized for 24 hours, the transfected cells were incubated under normoxia or hypoxia for 24 hours. Luciferase activities were measured and normalized to β-galactosidase activities. Each bar represents the mean + s.d. (n = 3) and * denotes $P < 0.05$ between the indicated groups.

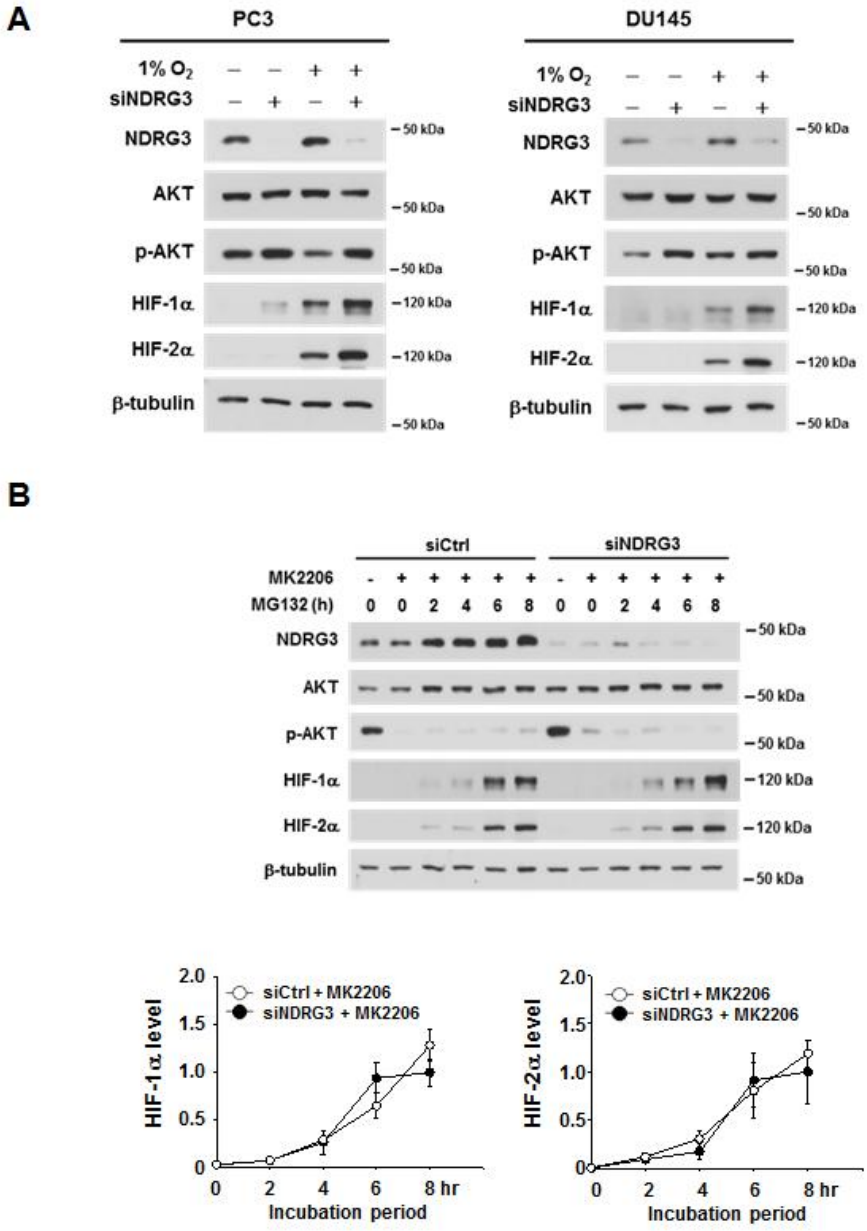
A
PC3
DU145
1% O2
siNDRG3
NDRG3
AKT
p-AKT
HIF-1α
HIF-2α
β-tubulin
50 kDa
120 kDa
B
siCtrl
siNDRG3
MK2206
MG132 (h)
0 0 2 4 6 8
siCtrl + MK2206
siNDRG3 + MK2206
HIF-1α level
HIF-2α level
Incubation period
0 2 4 6 8 hr

C

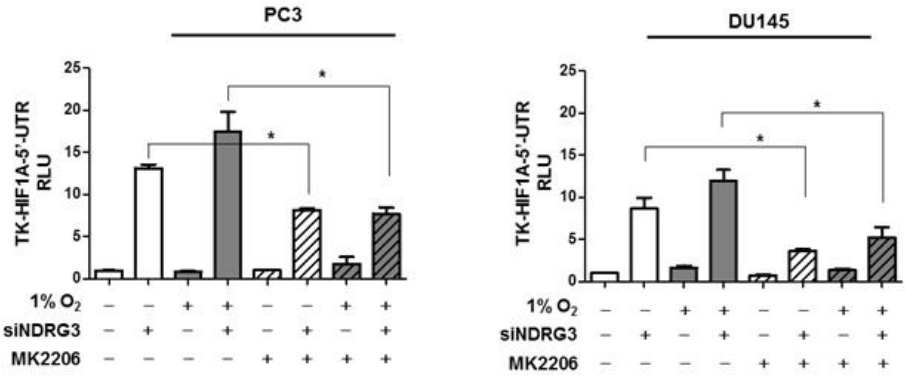

Fig. 8. NDRG3 suppresses phosphorylation of AKT.

(A) Phospho-AKT (S473) and total AKT levels were analyzed in PC3 and DU145 cells which were transfected with siNDRG3 and incubated under hypoxia for 24 hours. (B) The transfected PC3 or DU145 cells were pre-treated with 1 μM MK2206 for 16 hours, and incubated with 15 μM MG132 for the indicated times. Western blot intensities were analyzed using ImageJ and normalized to β-tubulin intensities. Each symbol represent the mean ± s.d. (n = 3). (C) The TK-HIF1A 5'UTR-luciferase reporter and the CMV-β-galactosidase plasmids were co-transfected with siCtrl or siNDRG3 into PC3 and DU145 cells. After stabilized for 24 hours, cells were incubated with DMSO or MK2206 under normoxia or hypoxia for 24 hours. Luciferase activities (means + s.d., n = 3) were normalized to β-galactosidase activities. * denotes $P < 0.05$ between the indicated groups.

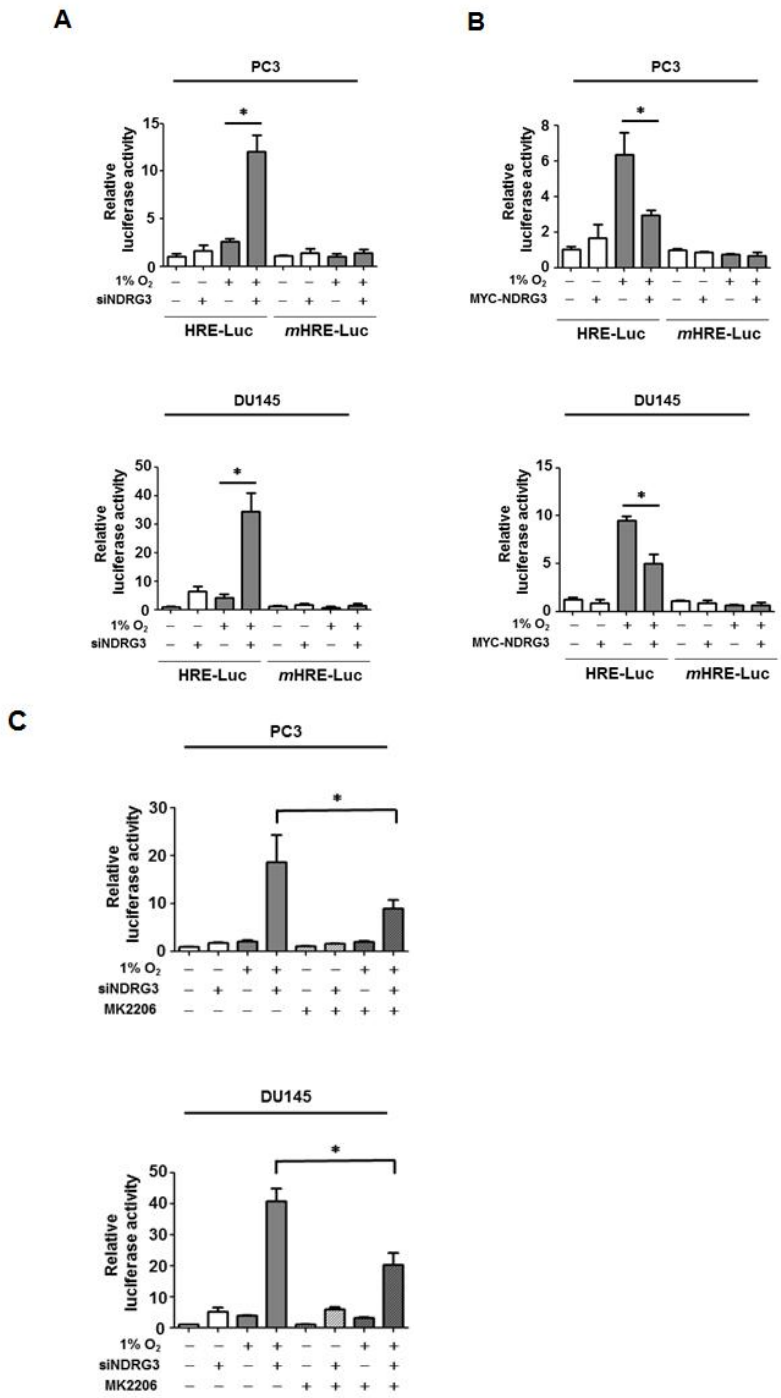
A
PC3
Relative luciferase activity
15
10
5
0
*
1% O2
siNDRG3
HRE-Luc
mHRE-Luc
DU145
50
40
30
20
10
0
B
PC3
8
6
4
2
MYC-NDRG3
DU145
C
PC3
30
20
MK2206
DU145

Fig. 9. NDRG3 attenuates the HIF-1-mediated HRE activation under hypoxia.

(A) PC3 and DU145 cells were co-transfected with the HRE- or mutated HRE-luciferase plasmid, the CMV-β-galactosidase plasmid and siCtrl or siNDRG3, and incubated under normoxia or hypoxia for 24 hours. (B) Cells were co-transfected with the reporter, the CMV-β-galactosidase and pcDNA or MYC-NDRG3 plasmids, and incubated under normoxia or hypoxia for 24 hours. (C) Cells were co-transfected with the HRE reporter plasmid, the β-galactosidase plasmid and siCtrl or siNDRG3. The cells were treated with DMSO or MK2206 and incubated under normoxia or hypoxia for 24 hours. Luciferase activities (means + s.d., $n = 3$) were normalized to β-galactosidase activities. * denotes $P < 0.05$ between the indicated groups.

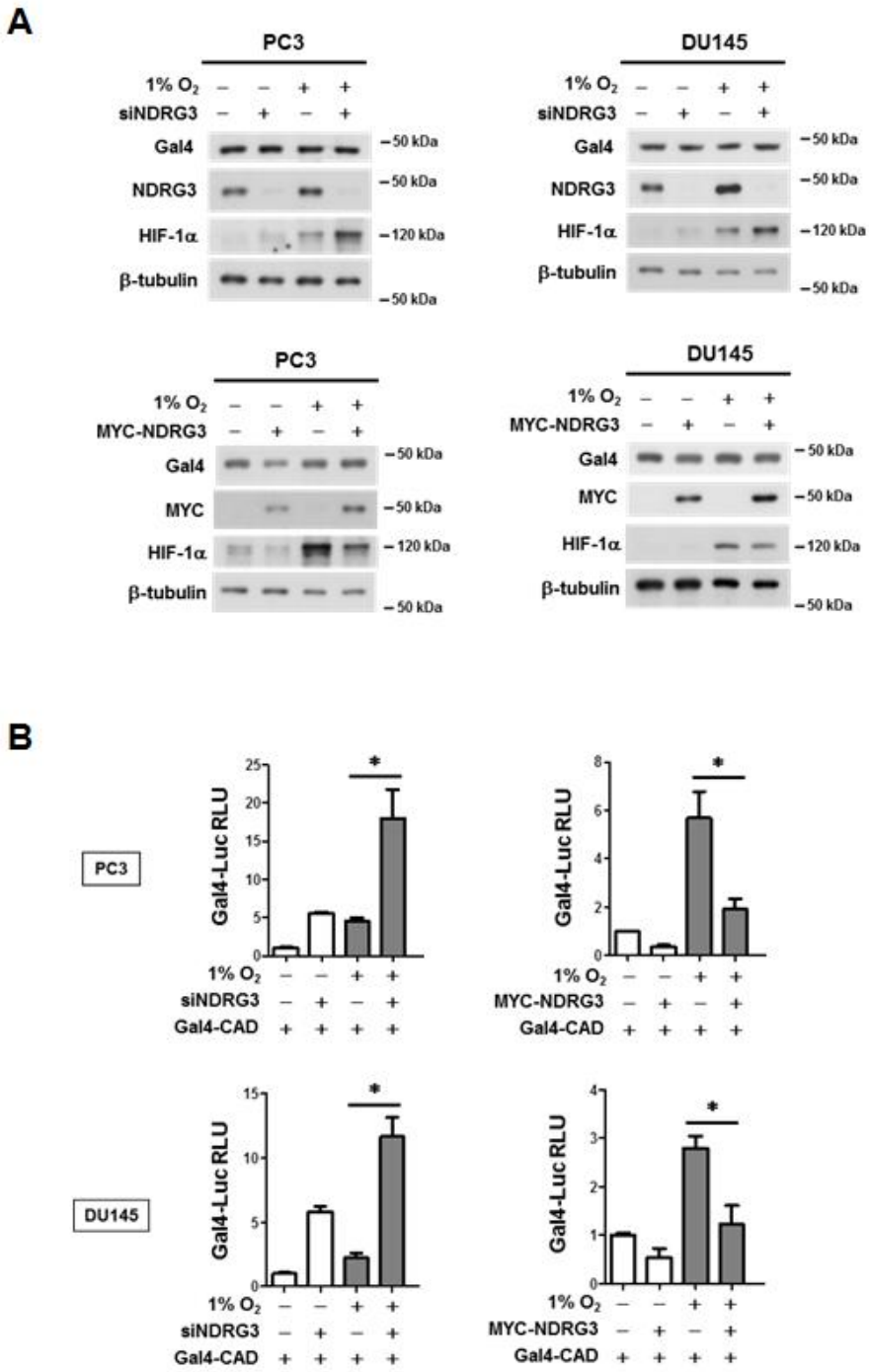
A
PC3
1% O2
siNDRG3
Gal4
NDRG3
HIF-1α
β-tubulin
50 kDa
120 kDa
DU145
MYC-NDRG3
MYC
B
Gal4-Luc RLU
Gal4-CAD
*

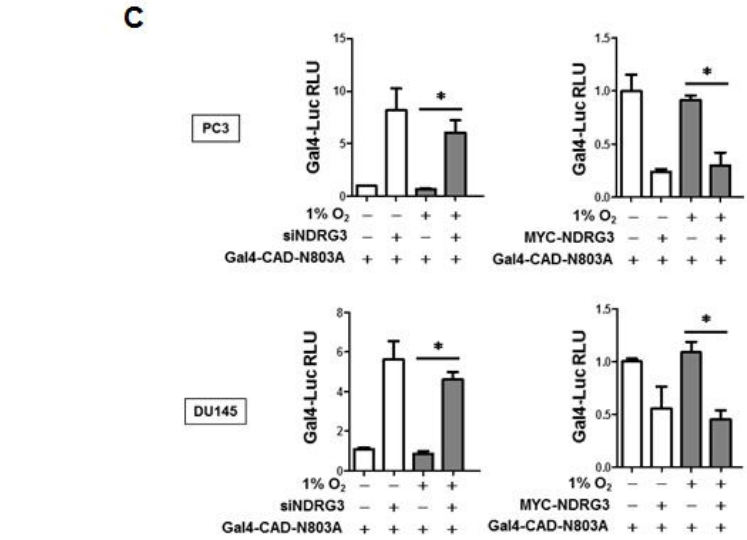
C
PC3
DU145
Gal4-Luc RLU
1% O2
siNDRG3
MYC-NDRG3
Gal4-CAD-N803A
*

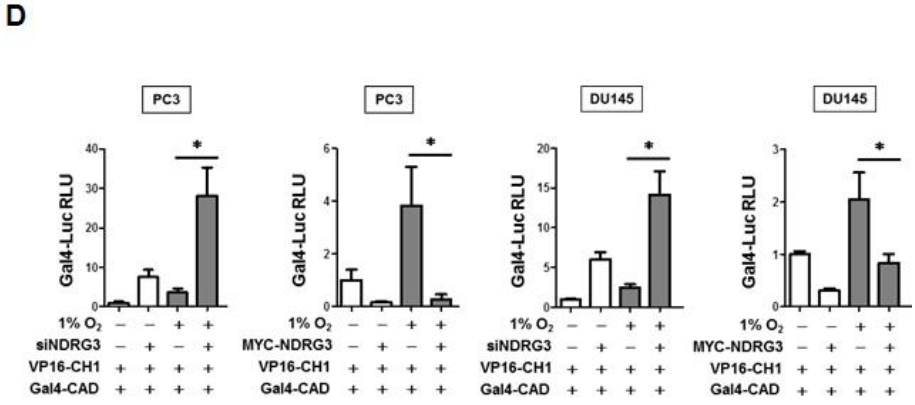
D
PC3
PC3
DU145
DU145
Gal4-Luc RLU
1% O2
siNDRG3
MYC-NDRG3
VP16-CH1
Gal4-CAD
*

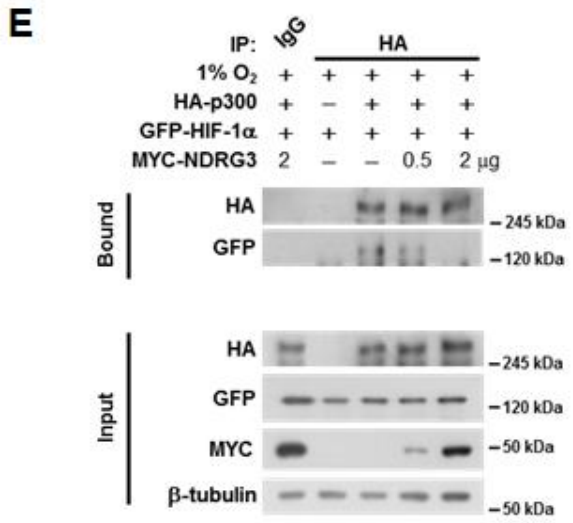

Fig. 10. NDRG3 represses the p300-dependent transcription of HIF-1α. (A,B) The MYC-NDRG3 plasmid or siNDRG3 was co-transfected with the Gal4 promoter-Luc reporter plasmid and the Gal4/DBD-HIF-1α_CAD plasmid or the Gal4/DBD-HIF-1α_CAD N803A plasmid into PC3 and DU145 cells. Cells were incubated under normoxia or hypoxia for 24 hours. (C) The MYC-NDRG3 plasmid or siNDRG3 was co-transfected with Gal4 promoter-Luc reporter, Gal4/DBD-HIF-1α_CAD and p300_CH1-VP16 plasmids. Cells were incubated under normoxia or hypoxia for 24 hours. Luciferase activities (means + s.d., n = 3) were normalized to β-galactosidase activities, and

presented as relative values to the normoxic control. * denotes $P < 0.05$ between the indicated group. (D) PC3 cells were co-transfected with GFP-HIF-1α, HA-p300, and MYC-NDRG3 (0.5 or 2 μg). Proteins in cell lysates were immunoprecipitated with anti-HA antibody and immunoblotted using the indicated antibodies. The experiments were performed three times.

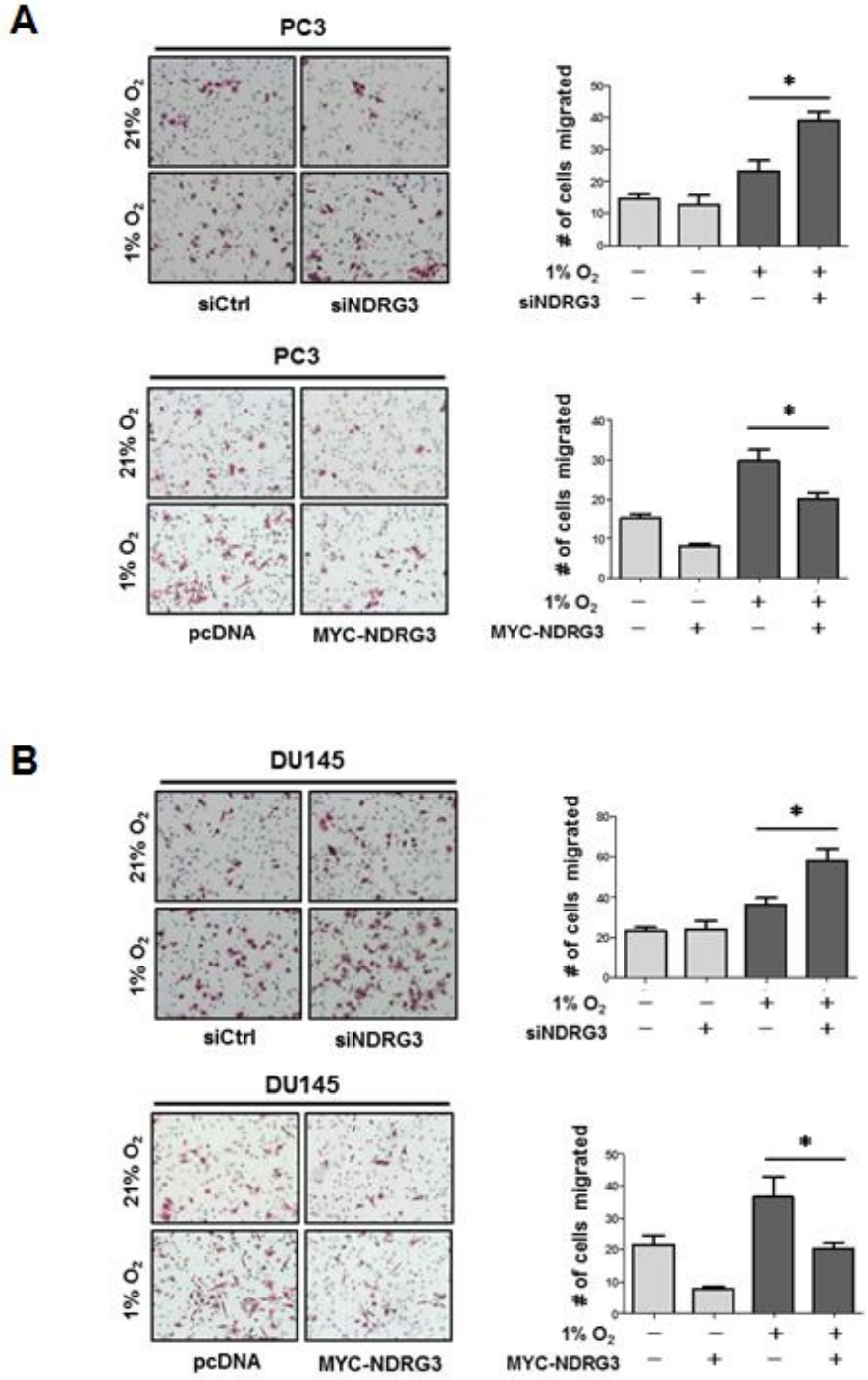
A
PC3
21% O2
1% O2
siCtrl
siNDRG3
# of cells migrated
1% O2
siNDRG3
PC3
pcDNA
MYC-NDRG3
MYC-NDRG3
B
DU145
DU145

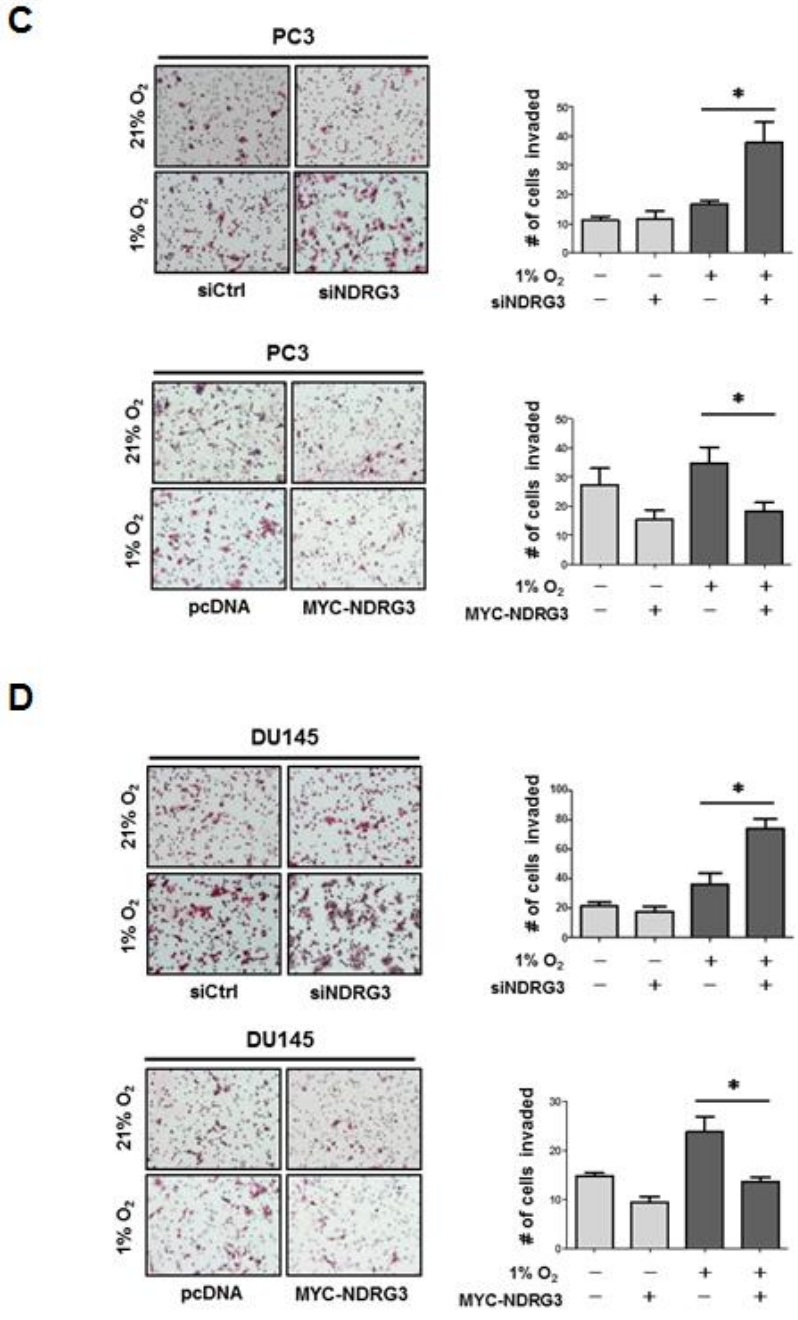
C
PC3
21% O2
1% O2
siCtrl
siNDRG3
# of cells invaded
*
1% O2
siNDRG3
PC3
21% O2
1% O2
pcDNA
MYC-NDRG3
# of cells invaded
*
1% O2
MYC-NDRG3
D
DU145
21% O2
1% O2
siCtrl
siNDRG3
# of cells invaded
*
1% O2
siNDRG3
DU145
21% O2
1% O2
pcDNA
MYC-NDRG3
# of cells invaded
*
1% O2
MYC-NDRG3

Fig. 11. NDRG3 functions to inhibit migration and invasion of prostate cancer cells.

PC3 (A,C) or DU145 (B,D) cells were transfected with siNDRG3 or MYC-NDRG3, and $1x10^4$ cells were seeded in a transwell culture plate. Upper chambers were filled with serum-free media and lower chambers with 10% FBS-containing media. Migration and invasion analyses were performed using uncoated and matrigel-coated interface membranes, respectively. After cells were incubated under normoxia or hypoxia for 24 hours, the membranes were fixed in 4% PFA and subjected to H&E staining. Representative images of each group are shown on the left, and the numbers (means +s.d. ,n = 3) of migrated or invaded cells are shown as bar graphs on the right. * denotes $P < 0.05$.

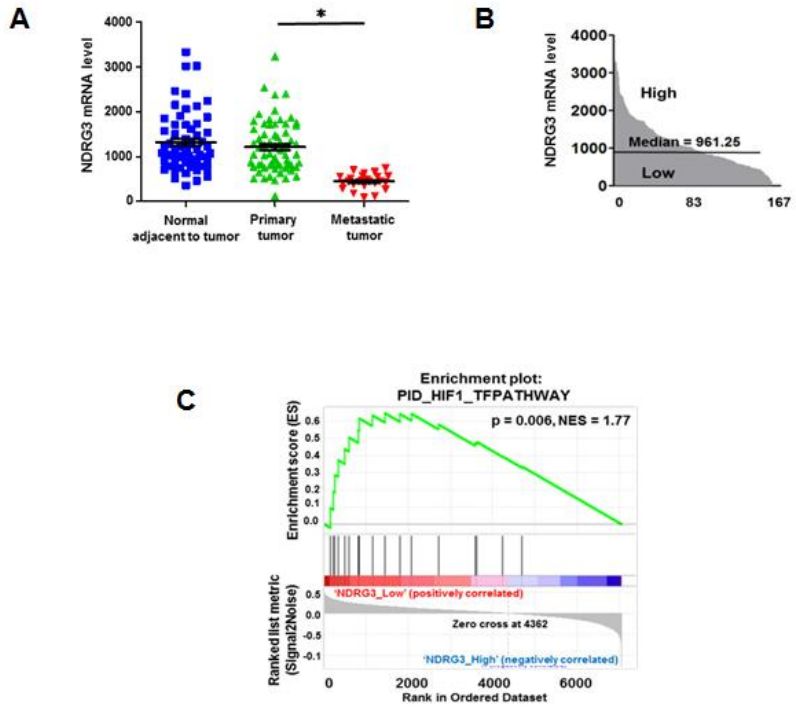

Fig. 12. NDRG3 expression is down-regulated in metastatic prostate cancer patients.

(A) Relative NDRG3 mRNA expressions in normal adjacent to tumor tissues (*n*=59), primary tumor tissues (*n*=66), metastatic tumor tissues (*n*=25), which were obtained from GEO data set GSE6919. (B) GSE6919 data set is divided into NDRG3_Low and NDRG3_High groups according to the median value (961.25) of the NDRG3 mRNA level. (C) GSEA enrichment plot for PID_HIF1_TFPATHWAY gene set

in NDRG3_Low group. The horizontal lines in all dot plots represent the means ± s.e.m. and * denotes $P < 0.05$ versus between the indicated groups.

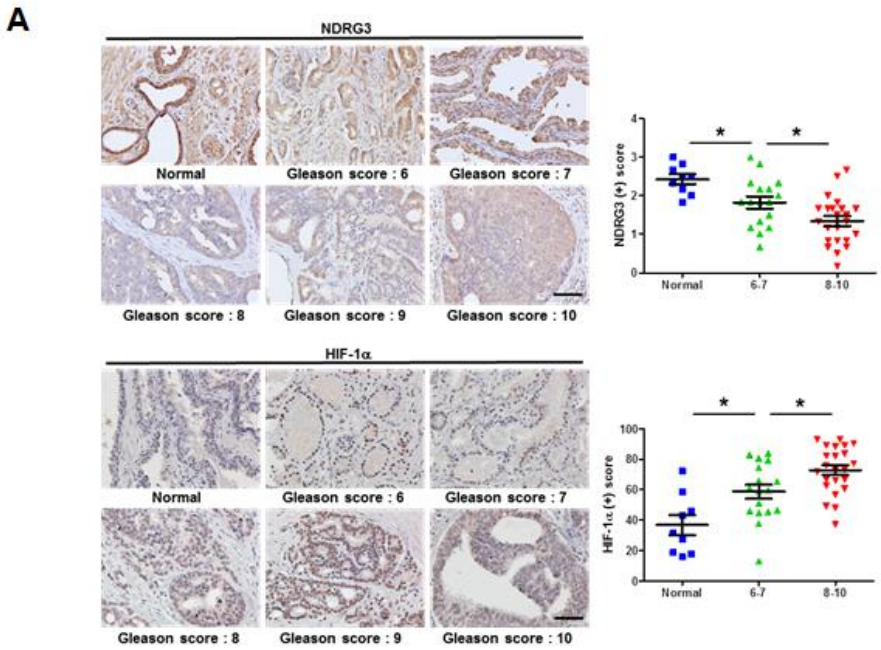
A
NDRG3
Normal
Gleason score : 6
Gleason score : 7
Gleason score : 8
Gleason score : 9
Gleason score : 10
NDRG3 (+) score
Normal
6-7
8-10
HIF-1α
HIF-1α (+) score

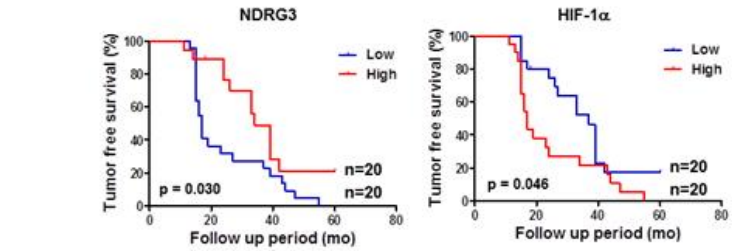
B
NDRG3
HIF-1α
Tumor free survival (%)
Low
High
n=20
n=20
p = 0.030
p = 0.046
Follow up period (mo)

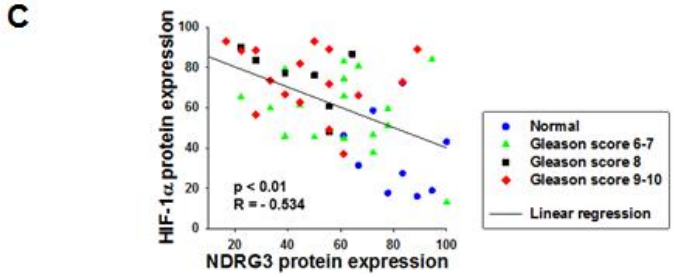
C
HIF-1α protein expression
NDRG3 protein expression
p < 0.01
R = - 0.534
Normal
Gleason score 6-7
Gleason score 8
Gleason score 9-10
Linear regression

Fig. 13. NDRG3 expression inversely correlates with prostate cancer progression and HIF-1α expression.

(A) IHC analyses of NDRG3 and HIF-1α protein expressions in human prostate adenocarcinoma tissue microarray. Representative images are shown on the left and dot plots of the immunostaining scores are shown on the right. The scale bar represents 50 μm. (B) Kaplan-Meier analysis for the association of NDRG3 or HIF-1α expressions and the tumor-free survival rates in human prostate adenocarcinoma tissue microarray. The Low and High groups were categorized according to the median values of the protein expressions. P-value was calculated by Log-rank Test. (C) Pearson correlation analysis shows negative correlation between NDRG3 and HIF-1α expressions in tissue microarray. R value indicates the Pearson correlation coefficient value. * denotes $P < 0.05$ versus between the indicated groups.

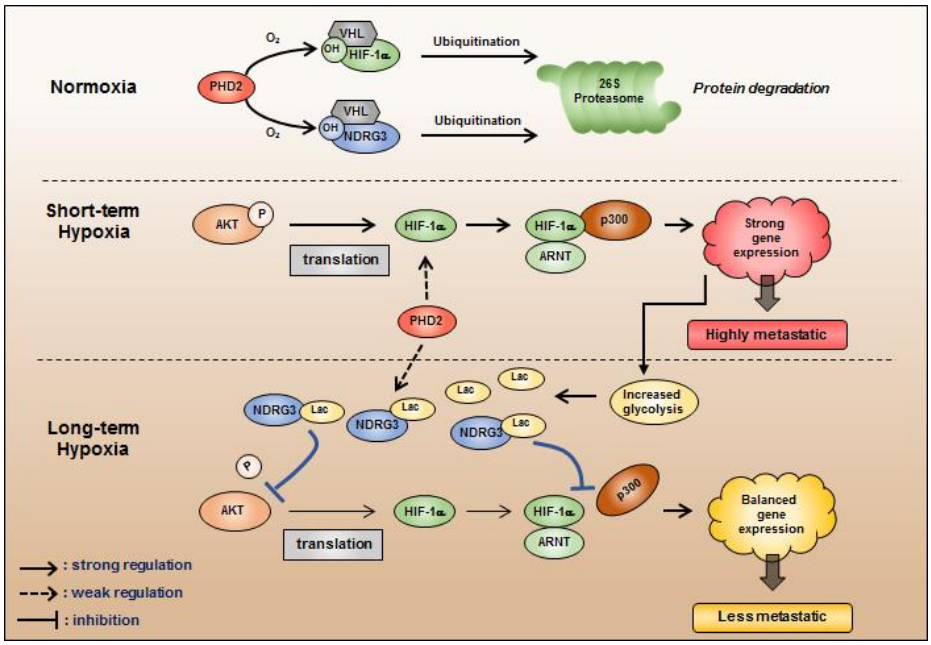

Fig. 14. Proposed hypothesis about the mechanism whereby NDRG3 counterbalances the HIF signaling pathway as a feed-back regulator. OH, hydroxylation; P, phosphorylation; Lac, lactate.

Table 1. Nucleotide sequences of primers used in RT-PCR.

Gene	Direction	Nucleotide Sequence
PDK1	Forward	5′-AACCCTCTAGGGAATACAGC-3′
	Reverse	5′-CCTTTGAGGAAAATTGACAG-3′
BNIP3	Forward	5′-TGTTGCAAGCTCAGAAGTAA-3′
	Reverse	5′-TTCTGAAAGTTTTCCTTCCA-3′
GAPDH	Forward	5′-TGTGGTCATGAGTCCTTCCA-3’
	Reverse	5’-CGAGATCCCTCCAAAATCAA-3’
HIF1A	Forward	5’-CCCAGATTCAGGATCAGACA-3’
	Reverse	5’-ACCATCATGTTCCATTTTTCG-3’
HIF2A	Forward	5’-TCATCATGTGTGAACCAATC-3’
	Reverse	5’-GAACACCACGTCATTCTTCT-3’

Table 2. Core enriched gene list for the gene set PID_HIF1_ TFPATHWAY

Probe	Gene Symbol	Gene Title	Rank in gene list	Rank metric score	Running ES	Core enrichment
HK2	HK2	hexokinase 2	156	0.353764	0.091885	Yes
NCOA1	NCOA1	nuclear receptor coactivator 1	225	0.328689	0.188197	Yes
HIF1A	HIF1A	hypoxia-inducible factor 1, alpha subunit (basic helix-loop-helix transcription factor)	261	0.318103	0.285788	Yes
RORA	RORA	RAR-related orphan receptor A	338	0.299635	0.371595	Yes
TFRC	TFRC	transferrin receptor (p90, CD71)	494	0.266397	0.435452	Yes
HK1	HK1	hexokinase 1	591	0.253815	0.503641	Yes
EGLN1	EGLN1	egl nine homolog 1 (C. elegans)	810	0.225232	0.545267	Yes
ETS1	ETS1	v-ets erythroblastosis virus E26 oncogene homolog 1 (avian)	830	0.223343	0.614579	Yes
NCOA2	NCOA2	nuclear receptor coactivator 2	1148	0.193335	0.631844	Yes
PFKFB3	PFKFB3	6-phosphofructo-2-kinase/fructose-2,6-biphosphatase 3	1445	0.16977	0.644497	Yes

Table 3. Patient information for the prostate cancer tissue array.

No.	Age	Sex	Organ	Diagnosis	Gleason score	Stage	Residual tumor	Follow-up month	Survival status	PSA (ng/ml)
1	60	Male	Prostate	adenocarcinoma	9	3	no	60	alive	11.2
2	64	Male	Prostate	adenocarcinoma	7	2b	no	60	alive	30
3	71	Male	Prostate	adenocarcinoma	9	3	yes	55	alive	60.4
4	64	Male	Prostate	adenocarcinoma	10	3	yes	47	alive	7.4
5	59	Male	Prostate	adenocarcinoma	9	3	yes	44	alive	9.8
6	65	Male	Prostate	adenocarcinoma	8	3	yes	43	alive	34.9
7	73	Male	Prostate	adenocarcinoma	7	2b	yes	42	alive	48.1
8	69	Male	Prostate	adenocarcinoma	7	2b	no	42	alive	10.6
9	62	Male	Prostate	adenocarcinoma	7	2b	yes	39	alive	37.3
10	66	Male	Prostate	adenocarcinoma	9	3	yes	39	alive	1.2
11	60	Male	Prostate	adenocarcinoma	9	3	yes	39	alive	40
12	66	Male	Prostate	adenocarcinoma	7	3	yes	39	alive	8.4
13	70	Male	Prostate	adenocarcinoma	7	3	yes	37	alive	7
14	65	Male	Prostate	adenocarcinoma	9	3	yes	23	dead	17.5
15	67	Male	Prostate	adenocarcinoma	9	3	yes	34	alive	13.1
16	69	Male	Prostate	adenocarcinoma	7	3	yes	33	alive	1.1
17	63	Male	Prostate	adenocarcinoma	9	3	yes	33	alive	11.8
18	69	Male	Prostate	adenocarcinoma	7	3	yes	27	alive	17.6
19	70	Male	Prostate	adenocarcinoma	7	3	yes	26	alive	9
20	58	Male	Prostate	adenocarcinoma	9	3	no	26	alive	5.8
21	58	Male	Prostate	adenocarcinoma	7	3	yes	24	alive	15.8
22	71	Male	Prostate	adenocarcinoma	7	2b	yes	24	alive	31.4
23	70	Male	Prostate	adenocarcinoma	7	3	yes	19	alive	14.4
24	59	Male	Prostate	adenocarcinoma	6	2a	no	18	alive	18.3
25	63	Male	Prostate	adenocarcinoma	9	3	yes	17	alive	16.6
26	72	Male	Prostate	adenocarcinoma	9	3	yes	16	alive	.
27	66	Male	Prostate	adenocarcinoma	8	2	yes	17	dead	10.8
28	70	Male	Prostate	adenocarcinoma	6	3	yes	16	alive	10.8
29	70	Male	Prostate	adenocarcinoma	7	2b	no	15	alive	.
30	68	Male	Prostate	adenocarcinoma	8	3	yes	15	alive	26.9

31	63	Male	Prostate	adenocarcinoma	10	3	yes	15	alive	.
32	57	Male	Prostate	adenocarcinoma	7	3	yes	15	alive	25
33	72	Male	Prostate	adenocarcinoma	8	2b	yes	15	alive	16.8
34	70	Male	Prostate	adenocarcinoma	8	3	yes	15	alive	0.5
35	75	Male	Prostate	adenocarcinoma	9	3	yes	15	alive	98
36	62	Male	Prostate	adenocarcinoma	9	3	yes	15	alive	.
37	63	Male	Prostate	adenocarcinoma	9	3	yes	14	alive	91
38	53	Male	Prostate	adenocarcinoma	9	3	yes	17	dead	161
39	63	Male	Prostate	adenocarcinoma	8	3	yes	13	alive	13
40	44	Male	Prostate	adenocarcinoma	7	3	yes	11	alive	.
41	69	Male	Prostate	normal	.	.	.	.	.	.
42	62	Male	Prostate	normal	.	.	.	.	.	.
43	66	Male	Prostate	normal	.	.	.	.	.	.
44	65	Male	Prostate	normal	.	.	.	.	.	.
45	69	Male	Prostate	normal	.	.	.	.	.	.
46	70	Male	Prostate	normal	.	.	.	.	.	.
47	70	Male	Prostate	normal	.	.	.	.	.	.
48	63	Male	Prostate	normal	.	.	.	.	.	.
49	44	Male	Prostate	normal	.	.	.	.	.	.

DISCUSSION

In spite of the numerous benefits of HIF-1α in hypoxic responses, a prolonged expression of HIF-1α eventually threatens cell survival during a long-term hypoxia because the pro-apoptotic genes are expressed by HIF-1α (Carmeliet *et al.*, 1998; Ginouves *et al.*, 2008; Greijer *et al.*, 2004). For this reason, it is reasonable that HIF-1α expression is robustly induced during acute hypoxia but gradually subsides at the late phase of hypoxia (Henze *et al.*, 2010; Uchida *et al.*, 2004). I also observed the downregulation of HIF-1α proteins in PC3 and DU145 cells after 16 hour hypoxia. In spite of many efforts, the mechanism underlying the temporal readjustment of HIF-1α expression has not been clearly understood. Based on my results, I can propose a new hypothesis on this mechanism. While hypoxia persists, HIF-1α expression is followed by NDRG3 expression because NDRG3 stabilization requires the lactate accumulation through HIF-1-induced glycolytic enzymes. After NDRG3 accumulates in cells, it does not only downregulate HIF-1α protein at the translational level, but also represses the transcriptional activity of HIF-1α at the epigenetic level. By doing so, NDRG3 controls the HIF-mediated cell migration and metastasis in prostate cancer. The proposed role of NDRG3 as a

feed-back regulator of HIF-1 is summarized in Fig. 14.

To date, several hypotheses have been proposed to explain how HIF-1α expression subsides for a long-term hypoxia. For instance, HSP70 recruits the chaperone-dependent E3 ubiquitin ligase CHIP (carboxyl terminus of Hsc70-interacting protein) to HIF-1α, leading to HIF-1α ubiquitination and degradation during prolonged hypoxia (Luo *et al.*, 2010). REST(repressor element 1-silencing transcription factor) or PRDX2/4 (peroxiredoxin 2 and 4) targets and inactivates the promoter of the HIF1A gene, which downregulates HIF-1α at the transcriptional level in prolonged hypoxia (Cavadas *et al.*, 2015; Luo *et al.*, 2016). PHD2/3, whose expressions are induced under hypoxia, facilitates the prolyl-hydroxylation of HIF-1α even under hypoxia and subsequently downregulates HIF-1α at the post-translational level (Minamishima *et al.*, 2009; Stiehl *et al.*, 2006). In this study, NDRG3 was also identified as a negative feed-back regulator of the HIF-mediated hypoxic signaling pathway. Given that the HIF-1 signaling is tightly controlled through multiple pathways, HIF-1 might be required for an emergency care of hypoxia-injured cells, but not for a long-term management of cell life.

NDRG3 has received a spot-light because its regulation is very similar to the oxygen-sensitive degradation of HIF-1α (Lee *et al.*, 2015). However, little is known about the role of NDRG3 in cellular adaptation to hypoxia. Lee et al. demonstrated that NDRG3 promoted angiogenesis, cell proliferation, and anti-apoptosis by activating the RAF-ERK pathway and that its expression is higher in hepatocellular carcinoma than in normal liver tissue (Lee *et al.*, 2015). According to the report, NDRG3 is considered to be oncogenic in liver cancer. On the contrary, a recent study showed that NDRG3 was downregulated in advanced breast cancer and that its expression positively correlated with increased disease-free survival rate (Estiar *et al.*, 2017). This report supports the tumor suppressive function of NDRG3 in breast cancer. Given such conflicting reports on NDRG3 function, NDRG3 may play differential roles in cancer progression depending on cell context. In this study, I found that NDRG3 inhibits migration and invasion of prostate cancer cells under hypoxia and that its expression inversely correlates with high cancer stage and poor prognosis. These results suggest that NDRG3 has a tumor-suppressive function in prostate cancer. The cancer type-dependent roles of NDRG3 remains to be further investigated.

In conclusion, my results revealed a novel mechanism of HIF-1α autoregulation through the cross-talk with hypoxia-inducible NDRG3. NDRG3 is induced by the HIF-1 signaling pathway, and in turn it blocks HIF-1α synthesis and also represses the transcriptional activity of HIF-1α. This study also provides new insight about the tumor-suppressive role of NDRG3 in prostate cancer. NDRG3 may be a potential target in developing a HIF-targeting anticancer strategy.

REFERENCES

Boddy,J.L.,Fox,S.B.,Han,C.,Campo,L.,Turley,H.,Kanga,S.,Malone,P.R.,Harris,A.L.,(2005)The androgen receptor is significantly associated with vascular endothelial growth factor and hypoxia sensing via hypoxia-inducible factors HIF-1α, HIF-2α, and the prolyl hydroxylases in human prostate cancer. *Clin Cancer Res* **11**, 7658-7663.

Carmeliet, P., Dor, Y., Herbert, J.M., Fukumura, D., Brusselmans, K., Dewerchin, M., Neeman, M., Bono, F., Abramovitch, R., Maxwell, P., *et al.*, (1998) Role of HIF-1alpha in hypoxia-mediated apoptosis, cell proliferation and tumour angiogenesis. *Nature* **394**, 485-490.

Cavadas, M.A., Mesnieres, M., Crifo, B., Manresa, M.C., Selfridge, A.C., Scholz, C.C., Cummins, E.P., Cheong, A., Taylor, C.T., (2015) REST mediates resolution of HIF-dependent gene expression in prolonged hypoxia. *Sci Rep* **5**, 17851.

Chun, Y.S., Choi, E., Kim, G.T., Lee, M.J., Lee, M.J., Lee, S.E., Kim, M.S., Park, J.W., (2000) Zinc induces the accumulation of hypoxia-inducible factor (HIF)-1alpha, but inhibits the nuclear

translocation of HIF-1beta, causing HIF-1 inactivation. *Biochem Biophys Res Commun* **268**, 652-656.

Estiar, M.A., Zare, A.A., Esmaeili, R., Farahmand, L., Fazilaty, H., Jafari, D., Samadi, T., Majidzadeh, A.K., (2017) Clinical significance of NDRG3 in patients with breast cancer. *Future Oncol* **13**, 961-969.

Ginouves, A., Ilc, K., Macias, N., Pouyssegur, J., Berra, E., (2008) PHDs overactivation during chronic hypoxia "desensitizes" HIFalpha and protects cells from necrosis. *Proc Natl Acad Sci U S A* **105**, 4745-4750.

Greijer, A.E., van der Wall, E., (2004) The role of hypoxia inducible factor 1 (HIF-1) in hypoxia induced apoptosis. *J Clin Pathol* **57**, 1009-1014.

Harris, A.L., (2002) Hypoxia--a key regulatory factor in tumour growth. *Nat Rev Cancer* **2**, 38-47.

Henze, A.T., Riedel, J., Diem, T., Wenner, J., Flamme, I., Pouyseggur, J., Plate, K.H., Acker, T., (2010) Prolyl hydroxylases 2 and 3 act in

gliomas as protective negative feedback regulators of hypoxia-inducible factors. *Cancer Res* **70**, 357-366.

Huang, L.E., Gu, J., Schau, M., Bunn, H.F., (1998) Regulation of hypoxia-inducible factor 1alpha is mediated by an O2-dependent degradation domain via the ubiquitin-proteasome pathway. *Proc Natl Acad Sci U S A* **95**, 7987-7992.

Imai, T., Horiuchi, A., Wang, C., Oka, K., Ohira, S., Nikaido, T., Konishi, I., (2003) Hypoxia attenuates the expression of E-cadherin via up-regulation of SNAIL in ovarian carcinoma cells. *Am J Pathol* **163**, 1437-1447.

Jaakkola, P., Mole, D.R., Tian, Y.M., Wilson, M.I., Gielbert, J., Gaskell, S.J., von Kriegsheim, A., Hebestreit, H.F., Mukherji, M., Schofield, C.J., *et al.*, (2001) Targeting of HIF-alpha to the von Hippel-Lindau ubiquitylation complex by O2-regulated prolyl hydroxylation. *Science* **292**, 468-472.

Kaelin, W.G., Jr., Ratcliffe, P.J., (2008) Oxygen sensing by metazoans: the central role of the HIF hydroxylase pathway. *Mol Cell* **30**, 393-402.

Khatua, S., Peterson, K.M., Brown, K.M., Lawlor, C., Santi, M.R., LaFleur, B., Dressman, D., Stephan, D.A., MacDonald, T.J., (2003) Overexpression of the EGFR/FKBP12/HIF-2alpha pathway identified in childhood astrocytomas by angiogenesis gene profiling. *Cancer Res* **63**, 1865-1870.

Lando, D., Peet, D.J., Gorman, J.J., Whelan, D.A., Whitelaw, M.L., Bruick, R.K., (2002a) FIH-1 is an asparaginyl hydroxylase enzyme that regulates the transcriptional activity of hypoxia-inducible factor. *Genes Dev* **16**, 1466-1471.

Lando, D., Peet, D.J., Whelan, D.A., Gorman, J.J., Whitelaw, M.L., (2002b) Asparagine hydroxylation of the HIF transactivation domain a hypoxic switch. *Science* **295**, 858-861.

Lee, D.C., Sohn, H.A., Park, Z.Y., Oh, S., Kang, Y.K., Lee, K.M., Kang, M., Jang, Y.J., Yang, S.J., Hong, Y.K., *et al.*, (2015) A lactate-induced response to hypoxia. *Cell* **161**, 595-609.

Lee, G.Y., Chun, Y.S., Shin, H.W., Park, J.W., (2016) Potential role of the N-MYC downstream-regulated gene family in reprogramming cancer metabolism under hypoxia. *Oncotarget* **7**, 57442-57451.

Luo, W., Chen, I., Chen, Y., Alkam, D., Wang, Y., Semenza, G.L., (2016) PRDX2 and PRDX4 are negative regulators of hypoxia-inducible factors under conditions of prolonged hypoxia. *Oncotarget* **7**, 6379-6397.

Luo, W., Zhong, J., Chang, R., Hu, H., Pandey, A., Semenza, G.L., (2010) Hsp70 and CHIP selectively mediate ubiquitination and degradation of hypoxia-inducible factor (HIF)-1alpha but Not HIF-2alpha. *J Biol Chem* **285**, 3651-3663.

Melotte, V., Qu, X., Ongenaert, M., van Criekinge, W., de Bruine, A.P., Baldwin, H.S., van Engeland, M., (2010) The N-myc downstream regulated gene (NDRG) family: diverse functions, multiple applications. *FASEB J* **24**, 4153-4166.

Minamishima, Y.A., Moslehi, J., Padera, R.F., Bronson, R.T., Liao, R.,

Kaelin, W.G., Jr., (2009) A feedback loop involving the Phd3 prolyl hydroxylase tunes the mammalian hypoxic response in vivo. *Mol Cell Biol* **29**, 5729-5741.

Qu, X., Zhai, Y., Wei, H., Zhang, C., Xing, G., Yu, Y., He, F., (2002) Characterization and expression of three novel differentiation-related genes belong to the human NDRG gene family. *Mol Cell Biochem* **229**, 35-44.

Schofield, C.J., Ratcliffe, P.J., (2004) Oxygen sensing by HIF hydroxylases. *Nat Rev Mol Cell Biol* **5**, 343-354.

Semenza, G.L., (1999) Regulation of mammalian O2 homeostasis by hypoxia-inducible factor 1. *Annu Rev Cell Dev Biol* **15**, 551-578.

Semenza, G.L., (2001) Hypoxia-inducible factor 1: oxygen homeostasis and disease pathophysiology. *Trends Mol Med* **7**, 345-350.

Semenza, G.L., (2003) Targeting HIF-1 for cancer therapy. *Nat Rev Cancer* **3**, 721-732.

Semenza, G.L., (2004) Hydroxylation of HIF-1: oxygen sensing at the molecular level. *Physiology (Bethesda)* **19**, 176-182.

Shaw, E., McCue, L.A., Lawrence, C.E., Dordick, J.S., (2002) Identification of a novel class in the alpha/beta hydrolase fold superfamily: the N-myc differentiation-related proteins. *Proteins* **47**, 163-168.

Shin, H.W., Cho, C.H., Kim, T.Y., Park, J.W., (2010) Sunitinib deregulates tumor adaptation to hypoxia by inhibiting HIF-1alpha synthesis in HT-29 colon cancer cells. *Biochem Biophys Res Commun* **398**, 205-211.

Shukla, S., Maclennan, G.T., Hartman, D.J., Fu, P., Resnick, M.I., Gupta, S., (2007) Activation of PI3K-Akt signaling pathway promotes prostate cancer cell invasion. *Int J Cancer* **121**, 1424-1432.

Stiehl, D.P., Wirthner, R., Koditz, J., Spielmann, P., Camenisch, G., Wenger, R.H., (2006) Increased prolyl 4-hydroxylase domain proteins

compensate for decreased oxygen levels. Evidence for an autoregulatory oxygen-sensing system. *J Biol Chem* **281**, 23482-23491.

To, K.K., Huang, L.E., (2005) Suppression of hypoxia-inducible factor 1alpha (HIF-1alpha) transcriptional activity by the HIF prolyl hydroxylase EGLN1. *J Biol Chem* **280**, 38102-38107.

Uchida, T., Rossignol, F., Matthay, M.A., Mounier, R., Couette, S., Clottes, E., Clerici, C., (2004) Prolonged hypoxia differentially regulates hypoxia-inducible factor (HIF)-1alpha and HIF-2alpha expression in lung epithelial cells: implication of natural antisense HIF-1alpha. *J Biol Chem* **279**, 14871-14878.

Wang, G.L., Jiang, B.H., Rue, E.A., Semenza, G.L., (1995) Hypoxia-inducible factor 1 is a basic-helix-loop-helix-PAS heterodimer regulated by cellular O2 tension. *Proc Natl Acad Sci U S A* **92**, 5510-5514.

Yang, M.H., Wu, K.J., (2008a) TWIST activation by hypoxia inducible factor-1 (HIF-1): implications in metastasis and development. *Cell Cycle*

7, 2090-2096.

Yang, M.H., Wu, M.Z., Chiou, S.H., Chen, P.M., Chang, S.Y., Liu, C.J., Teng, S.C., Wu, K.J., (2008b) Direct regulation of TWIST by HIF-1alpha promotes metastasis. *Nat Cell Biol* **10**, 295-305.

Zhong, H., Agani, F., Baccala, A.A., Laughner, E., Rioseco-Camacho, N., Isaacs, W.B., Simons, J.W., Semenza, G.L., (1998) Increased expression of hypoxia inducible factor-1alpha in rat and human prostate cancer. *Cancer Res* **58**, 5280-5284.

Zhong, H., Chiles, K., Feldser, D., Laughner, E., Hanrahan, C., Georgescu, M.M., Simons, J.W., Semenza, G.L., (2000) Modulation of hypoxia-inducible factor 1alpha expression by the epidermal growth factor/phosphatidylinositol 3-kinase/PTEN/AKT/FRAP pathway in human prostate cancer cells: implications for tumor angiogenesis and therapeutics. *Cancer Res* **60**, 1541-1545.

Zhou, R.H., Kokame, K., Tsukamoto, Y., Yutani, C., Kato, H., Miyata, T., (2001) Characterization of the human NDRG gene family: a newly

identified member, NDRG4, is specifically expressed in brain and heart. *Genomics* **73**, 86-97.

국 문 초 록

저산소 유도인자 (HIFs)와 N-MYC downstream-regulated gene 3 (NDRG3)는 prolyl-hydroxylase domain enzymes (PHDs)에 의하여 산소 의존적으로 단백질 발현이 조절된다. 세포의 저산소 적응과정에서 HIF의 역할은 매우 잘 알려진 반면, NDRG3의 역할은 알려진 것이 적다. 본 논문에서는 전립선 암 세포의 저산소 적응 과정에서 NDRG3의 역할에 대하여 연구하였다. 저산소에서 NDRG3 단백질의 축적은 HIF-1/2α의 발현보다 더 이후에 이루어짐을 관찰하였고 NDRG3가 AKT-의존적 HIF1A mRNA 번역을 억제시킴을 밝혔다. 나아가 NDRG3는 HIF-1α와 그의 co-activator인 p300간의 결합을 방해함으로써 HIF-1α의 전사기능을 감소시켰고 이는 NDRG3가 장기적인 저산소 환경에서 세포의 생존율을 높이기 위하여 HIF-1 신호전달 체계를 조절할 가능성을 제시하였다. HIF-1α가 주관하는 다양한 세포 반응 중에서 저산소 환경의 세포 이동에 집중하여 연구하였다. Transwell chamber를 이용한 세포 이동 실험에서 NDRG3가 전립선 암 세포의 저산소 세포 이동과 침투를 억제하는 것을 밝혔다. GEO database를 이용한 bioinformatics 분석을 통해서 NDRG3 mRNA 발현이 전립선 암 전이 조직에서 감소되어 있고 NDRG3의 mRNA발현이 낮을수록 HIF-1 하위전자들이 증가한다는 것을 밝혔다. 실제로 전립선 암 환자 조직 microarray 분석을 통해 Gleason 점수 8 이상의 환자 조직에서 NDRG3의 단백질 발현이 감소되어 있고 NDRG3의 발현

이 낮은 환자 집단에서 무병 생존율이 유의미하게 낮으며 HIF-1α의 발현과는 부적 상관의 관계임을 밝혔다. 따라서 본 연구는 NDRG3가 저산소 환경에서 전립선 암 세포의 전이를 억제하는 기능을 하고 있음을 밝혔다.

Key words: **hypoxia, HIF-1α, prostate cancer, NDRG3, AKT, metastasis**

Student Number: **2015-23242**